

## **Certification**

### **Surface Films: Do they Influence the Effectiveness of Oil Spill Chemical Dispersants as Studied in a Wave Tank Facility?**

by

Thomas L. King

A Thesis Submitted to Saint Mary's University, Halifax, Nova Scotia,  
in Partial Fulfillment of the Requirements for the  
Degree of Master of Science in Applied Science

May 2011, Halifax, Nova Scotia

Copyright Thomas L. King, 2011

Approved: Dr. Jason Clyburne  
Supervisor  
Department of Chemistry &  
Environmental Studies Program

Approved: Dr. Gerrard Marangoni  
External Examiner  
Department of Chemistry  
St. Francis Xavier University

Approved: Dr. Kenneth Lee  
Supervisory Committee Member  
Department of Fisheries & Oceans

Approved: Dr. Kathy Singfield  
Supervisory Committee Member  
Department of Chemistry

Approved: Dr. Jason Masuda  
Program Representative

Approved: Dr. Marc Lamoureux  
Graduate Studies Representative

Date: May 13, 2011



Library and Archives  
Canada

Published Heritage  
Branch

395 Wellington Street  
Ottawa ON K1A 0N4  
Canada

Bibliothèque et  
Archives Canada

Direction du  
Patrimoine de l'édition

395, rue Wellington  
Ottawa ON K1A 0N4  
Canada

*Your file* *Votre référence*  
ISBN: 978-0-494-79982-6  
*Our file* *Notre référence*  
ISBN: 978-0-494-79982-6

#### NOTICE:

The author has granted a non-exclusive license allowing Library and Archives Canada to reproduce, publish, archive, preserve, conserve, communicate to the public by telecommunication or on the Internet, loan, distribute and sell theses worldwide, for commercial or non-commercial purposes, in microform, paper, electronic and/or any other formats.

The author retains copyright ownership and moral rights in this thesis. Neither the thesis nor substantial extracts from it may be printed or otherwise reproduced without the author's permission.

---

In compliance with the Canadian Privacy Act some supporting forms may have been removed from this thesis.

While these forms may be included in the document page count, their removal does not represent any loss of content from the thesis.

#### AVIS:

L'auteur a accordé une licence non exclusive permettant à la Bibliothèque et Archives Canada de reproduire, publier, archiver, sauvegarder, conserver, transmettre au public par télécommunication ou par l'Internet, prêter, distribuer et vendre des thèses partout dans le monde, à des fins commerciales ou autres, sur support microforme, papier, électronique et/ou autres formats.

L'auteur conserve la propriété du droit d'auteur et des droits moraux qui protègent cette thèse. Ni la thèse ni des extraits substantiels de celle-ci ne doivent être imprimés ou autrement reproduits sans son autorisation.

---

Conformément à la loi canadienne sur la protection de la vie privée, quelques formulaires secondaires ont été enlevés de cette thèse.

Bien que ces formulaires aient inclus dans la pagination, il n'y aura aucun contenu manquant.

  
**Canada**

## **Abstract**

Surface Films: Do they Influence the Effectiveness of Oil Spill Chemical Dispersants as Studied in a Wave Tank Test Facility?

by Thomas L. King

Abstract: Lab basins and wave tanks have unnatural boundaries (walls) that provide an ideal environment for surface film formation on seawater. Surface films form from natural surfactants in oil and dispersant overspray when applied to seawater. The adsorption process of selected crude oils, Arabian Light (ALC) and Alaskan North Slope (ANS) on static seawater in a lab basin was demonstrated to follow diffusion-controlled short time limit adsorption kinetics. The process of crude oil spreading on the surface of the basin seawater was affected in the presence of surface films as shown using kinetic models. ANS dispersed in the dynamic wave tank seawater with and without a surface film (dispersant overspray) was evaluated using kinetic models. It was found that oil dispersed in wave tank seawater, in the presence of dispersant overspray, influences oil dispersant effectiveness and produced confounding outcomes that are an unnatural model of dispersed oil fate and effects.

May 13, 2011

## **Dedication**

**in memory of my Dad**  
(Charles Henry King)

## **Acknowledgements**

Funding for this research was supported by the Department of Fisheries and Ocean Canada, the Centre for Offshore Oil, Gas and Energy Research (COOGER) in collaboration with Saint Mary's University. Dr. J.A.C. Clyburne thanks the Natural Sciences and Engineering Research Council and the Canada Research Chairs Program for financial support.

I am extremely grateful to my advisor, Dr. Jason Clyburne, for his guidance, support and encouragement throughout my research and studies at Saint Mary's University. I would like to thank Dr Kathy Singfield for serving as a co-supervisor, for reviewing this work, and for her advice on some of the physical chemical aspects of my thesis. Also, I would like to thank Dr Kenneth Lee for his continuous support and encouragement as a co-supervisor for my Masters thesis and as my supervisor while working full-time with the Centre for Offshore Oil, Gas and Energy Research of the Department of Fisheries and Oceans (DFO). Ken has graciously permitted me the opportunity to further my educational studies later in life in order to offer a better opportunity to advance in my career with DFO. I would like to extend special thanks to all the chemistry staff and other members of the COOGER team for their support and aid throughout my thesis research.

I would like to thank my wife Laura, my daughter Caroline, and my son Raleigh for their support and patience while I was attaining my graduate degree.

## List of Terms and Abbreviations

$\gamma$	Interfacial or Surface Tension
$\eta$	Viscosity
$\gamma(t)$	Surface Tension at Time ( $t$ )
$\gamma_0$	Initial Surface Tension
$^{\circ}\text{C}$	Degree Celsius
$^{\circ}\text{K}$	Degrees Kelvin
$\mu\text{L}$	Microlitre
$\mu\text{m}$	Micrometres
ALC	Arabian Light Crude
ANS	Alaskan North Slope Crude Oil
API gravity	American Petroleum Institute Gravity
cm	Centimetres
$C_0$	Initial Concentration
$D$	Diffusion Coefficient
DOR	Disperant-to-Oil Ratio
g	Grams
GC	Gas Chromatography
$h_0$	Initial Oil Thickness
$h_{ss}$	Terminal (Steady-State) Oil Thickness
$h_t$	Oil Thickness at Time ( $t$ )
Hz	Hertz
IFO 120	Intermediate Fuel oil 120

$m$	.....	Metres
min	.....	Minutes
mL	.....	Millilitres
mm	.....	Millimetres
$m_o$	.....	Initial Mass
ms	.....	Milliseconds
$m_{ss}$	.....	Terminal Mass (Steady-State)
$m_t$	.....	Mass at Time (t)
nm	.....	Nanometres
ppm	.....	Parts-Per-Million
$r$	.....	Radius
$R$	.....	Ideal Gas Constant
$r^2$	.....	Coefficient of Variance
$R_l$	.....	Radius of Oil Lens
$R_r$	.....	Reaction Rate
$s$	.....	Seconds
$T$	.....	Temperature
$V$	.....	Volume
$\rho$	.....	Density

# Table of Contents

<b>Abstract</b> .....	2
<b>Dedication</b> .....	3
<b>Acknowledgements</b> .....	4
<b>List of Terms and Abbreviations</b> .....	5
<b>Table of Contents</b> .....	7
<b>List of Tables</b> .....	10
<b>List of Figures</b> .....	11
<b>Chapter 1</b> .....	13
<b>Introduction</b> .....	13
<i>1.1 Objectives</i> .....	18
<b>Chapter 2</b> .....	19
<b>Literature Review</b> .....	19
<i>2.1 Importance of Dispersants</i> .....	19
<i>2.2 Dispersant-Effectiveness Tests</i> .....	20
<i>2.3 Factors Affecting Dispersant Effectiveness</i> .....	24
<i>2.4 Recommended Research and Potential Problems</i> .....	26
<i>2.5 Research Questions/Recommendations</i> .....	27
<i>2.5.1 Will Surface Films Form During Oil/Oil Dispersant Application to Seawater in a Static Environment?</i> .....	28
<i>2.5.2 What Effect Do Surface Films on the Seawater Surface Have on the Oil Spreading Rate in a Static Environment?</i> .....	28

2.5.3 <i>What Affect Do Surface Films (Contaminated Seawater) Have on the Oil Dispersant Effectiveness Tests in a Dynamic Wave Tank?</i> .....	31
<b>Chapter 3</b> .....	31
<b>Experimental Description</b> .....	31
3.1 <i>Oil Characterization and Dispersant Information</i> .....	32
3.2 <i>Adsorbed Film Formation (Basin Tests)</i> .....	33
3.3 <i>Kinetic Investigations of Oil Spreading</i> .....	34
3.4 <i>Surface Film Impacts on Dispersant Effectiveness (Wave Tank)</i> .....	36
3.41 <i>Wave Tank Operations</i> .....	37
3.42 <i>Natural Attenuation of Oil and Oil Treated with Dispersant</i> .....	38
3.43 <i>Created Surface Film and Chemical Dispersion of Oil</i> .....	38
3.44 <i>Lab Analysis of Disperse Oil Water Samples</i> .....	39
<b>Chapter 4</b> .....	41
<b>Results and Discussion</b> .....	41
4.1 <i>Oil Characterization</i> .....	41
4.2 <i>Surface Tension Measurements and Instrument Calibration</i> .....	42
4.3 <i>Interfacial Tension Gradients Formed on Basin Seawater</i> .....	43
4.4 <i>Interfacial Tension Gradient Effects on Oil Spreading Rate</i> .....	47
4.5 <i>The Effect of Oil Dispersant Overspray on Oil Dispersant Effectiveness</i> .....	53
<b>Chapter 5</b> .....	67

<b>Summary and Conclusions</b> .....	67
<i>5.1 Surface Film Formation</i> .....	67
<i>5.2 Oil Spreading Rates</i> .....	68
<i>5.3 Oil Dispersant Effectiveness</i> .....	69
<b>Bibliography</b> .....	71
<b>Appendix A</b> .....	75
<b>Supporting Data</b> .....	75
<b>Appendix B</b> .....	94
<b>Example Calculations</b> .....	94

## **List of Tables**

<b>Table 4-1:</b> Physical & chemical compositions of oils used in the study.....	42
<b>Table 4-2:</b> Experimental conditions and regression analysis on oil spreading kinetics...	49
<b>Table 4-3:</b> Wave tank experimental conditions .....	54
<b>Table 4-4:</b> First order kinetics data for chemically dispersed oil.....	63

## List of Figures

<b>Figure 2-1:</b> Schematic diagram of the wave tank (all units are in cm). .....	23
<b>Figure 2-2:</b> Photographs of the wave tank showing the different types of waves generated: A) transverse B) spilling breakers and C) plunging breakers .....	24
<b>Figure 2-3:</b> Schematic representation of the wave tank flow-through system (not to scale, Li et al., 2009). .....	24
<b>Figure 3-1:</b> A photo of the bab basin used for diffusion and oil spreading studies. ....	34
<b>Figure 3-2:</b> A photo of a created controlled surface film in the wave tank. ....	39
<b>Figure 4-1:</b> A plot of interfacial tension as a function of the natural logarithm of dispersant concentration.....	43
<b>Figure 4-2:</b> A plot of interfacial tension as a function of elapsed time indicating surface film formation from A) oil & B) oil/dispersant applied to basin seawater. ....	44
<b>Figure 4-3:</b> A plot of viscosity as a function of elapsed time A) oil & B) oil/dispersant applied to basin seawater. ....	45
<b>Figure 4-4:</b> A plot of interfacial tension as a function of the square root of time ( $s^{1/2}$ ) for ALC & ANS. ....	46
<b>Figure 4-5:</b> A plot of Lens growth and oil thickness decay as a function of time A) ANS spreading on clean seawater, B) ANS spreading on seawater with surface film, C) IFO 120 spreading on clean seawater, and D) IFO 120 spreading on seawater with surface film.....	50
<b>Figure 4-6:</b> Logarithmic plots of the spreading kinetics of oil on clean seawater and seawater with surface film A) ANS and B) IFO 120.....	52
<b>Figure 4-7:</b> First order kinetics plots of ANS spreading on A) clean seawater & B).....	52

**Figure 4-8:** First order kinetics plots of IFO 120 spreading on A) clean seawater & B) seawater with a surface film. .... 53

**Figure 4-9:** Temporal and spatial plots of average (n=3) hydrocarbon and interfacial tension levels 6m from oil release: A) ANS naturally attenuated; B) ANS dispersed with Corexit 9500; and C) surface film interference/ANS Dispersed with Corexit 9500. .... 56

**Figure 4-10:** Temporal and spatial plots of average (n=3) hydrocarbon and interfacial tension levels 10m from oil release: A) ANS naturally attenuated; B) ANS dispersed with Corexit 9500; and C) surface film interference/ANS Dispersed with Corexit 9500. .... 57

**Figure 4-11:** Photos of visual observations: A) intense oily sheen formation of chemically dispersed oil with surface film interference, B) chemical dispersion of oil, and C) natural attenuation of oil. .... 59

**Figure 4-12:** GC-FID chromatograms A) naturally dispersed oil, B) chemically dispersed oil, C) chemically dispersed oil in presence of surface films, D) ANS standard and E) 25 ppm Corexit 9500 in seawater. .... 61

**Figure 4-13:** 1<sup>st</sup> Order kinetics plot of dispersed oil in wave tank seawater with/without surface film interference. .... 64

**Figure 4-14:** A plot of interfacial tension as a function of the square root of time ( $s^{1/2}$ ) for dispersed oil & dispersed oil with horizontal interfacial gradient interference (A) surface and (B) subsurface. .... 66

# Chapter 1

## Introduction

Offshore oil and gas development, the transport of large volumes of oil across seas, and the recent oil spill in the Gulf of Mexico (April, 2010) have stimulated a growing global interest in the use of chemical dispersants to remediate accidental oil spills at sea. Over the past decade, this interest has been motivated by the development of a number of new commercially available dispersants, such as Corexit 9500, all of which are commonly considered to be non-toxic to marine life. These dispersants have been reported to be effective at dispersing heavy oils (Intermediate fuel oil 120&180) that were believed to be non-dispersible in the past (Lessard & Demarco, 2000).

Oil is immiscible with seawater. The fate of surface spilled oil or accidentally released oil from water depths is also at the water surface where it exists finally as a thin film. This layer of oil acts as a barrier to the natural processes of oxygen exchange. Moreover, the native microbial population have access to larger oil droplets that require more time to degrade. In order to lessen the impact of an oil spill or release on coastal and marine areas it becomes imperative to first physically break-up the continuous oil lens into tiny droplets. This discontinuous oil layer can then permit the increase of oxygen transport across the air/water boundary, thus encouraging biodegradation of the oil by micro-organisms (Kanicky, Lopez-Montilla, Pandey, and Shah, 2001). This is achieved by applying dispersant (surfactant) to the oil.

Surfactants have a hydrophilic (water-loving) head and a lipophilic (oil-loving) tail. Surfactants are thus compatible with both oil and water, effectively reducing the interfacial tension at the oil-seawater interface. Dispersants, like Corexit 9500 are

surfactant based solutions that are designed to disperse oil on seawater. When dispersants are applied the oil slick disperses into droplets (ideally  $<70 \mu\text{m}$ ) with continuous wave energy (Li et al., 2008a). This process removes the oil from the seawater surface to the subsurface where it can be transported by waves and current thus reducing impacts to coastal areas. This process is called an emulsion, because it involves the dispersion of one immiscible liquid (oil) in another (seawater) (Schamm, 2005). This ultimately contributes to the weathering process where there is interaction with sediment thus sinking the oil. Also, the small droplet size ( $<70 \mu\text{m}$ ) provides an ideal environment for micro-organisms to surround the dispersed oil droplets and ingest them as a source of energy thus encouraging bio-degradation.

The successful application of dispersants to break-up the oil slicks has been demonstrated through a multitude of evaluations tests in the laboratory, in field mesocosm trials, and application of dispersants on actual spills (Sterling et al., 2004; Venosa et al., 2002; & Li et al., 2008b). Sea trials would be the ideal scenario; however they are very expensive and there is the risk of environmental impacts. Lab-scale tests are not considered to be effective models of the real, large-scale problem thus encouraging the development of large-scale sea-model facilities such as, wave tanks (Sterling et al., 2004; Venosa et al., 2002). These facilities are capable of simulating natural wave energies to assist in the evaluation of chemical dispersant use on oil spills at sea (Li et al., 2008b).

Dispersants are surface active agents. Cleaning agents like 'Big Orange' contain surfactants. The introduction of unwanted residual surfactants from cleaning agents may be creating or contributing to the creation of a film of surfactant molecules at the

seawater surface. They would be distributed between the surface of the water (or the air/water interface) as a surface film and the bulk of the water (as monomers). If their concentration is high enough, they might be distributed between the surface of the water as a surface film and the bulk of the water as micelles. After the application of the crude oil, these same surfactant molecules may be creating or contributing to the creation of a film of surfactant molecules now adsorbed at the oil-water interface. They may also be in the form of emulsion (trapping oil in a detergent sort-of way) in the bulk of the water. However, if properly designed cleaning procedures are followed and the seawater is tested prior to operations then surfactants from cleaning should not be an issue.

There may also be some unwanted biofilms in the tank. Biofilms adsorb onto the surface of the water. After the application of the crude oil, the biofilm would be miscible with the phase and contribute to the crude oil slick. Naturally occurring biofilms can form in the testing facility tanks and interfere with the control variables by bio-degrading the dispersed oil samples collected to evaluate oil dispersant efficiency. This issue can be prevented by either immediately extracting the seawater samples after oil dispersant studies or preserving the samples with acid to destroy the micro-organisms prior to sample storage.

Adsorption is an entropically driven process where molecules diffuse preferentially from a bulk phase (oil) to the water interface (Kanicky et al., 2001). In this reference, Kanicky is specifically describing the event of crude oil coming into contact with seawater. Moreover, this is crude oil that contains naturally-occurring surfactant molecules. He is thus describing the specific adsorption of these naturally-occurring surfactant molecules from the bulk oil phase to the oil-water interface. As he notes, these

surfactants accumulate at the (oil-water) interface and form an adsorbed film (surface film), which lowers the interfacial tension between the two liquids, oil and water.

If the isolated surfactant were added to just oil, there would be an equilibrium established between the surfactant monomer in the oil (bulk – either existing as a micelle or as a single monomer depending on the concentration) and the adsorbed surfactant (film) on the surface of the oil, i.e., at the oil/air interface. The hydrophobic part of the surfactant molecule would be pointing downward freely into the oil.

If the isolated surfactant were added to just water, there would be an equilibrium established between the surfactant monomer in the water (bulk – either existing as a micelle or as a single monomer – depending on the concentration) and the adsorbed surfactant (surface film) on the water at air/water interface. Here, the hydrophilic parts of the surfactant would be freely pointing downward into the water. There would, of course, be a reduction in the surface tension of the water as the presence of the adsorbed surfactant would reduce the number of water molecules at the surface of the water.

Gibbs free energy ( $G$ ) is defined as  $G=H-TS$ , where  $H$  is enthalpy,  $T$  is temperature and  $S$  is entropy (Ip & Toguri, 1994; Schamm, 2005). It would seem that taking a molecule from the bulk to the surface would be accompanied by a relative decrease in the measure of its disorder that is, a decrease in entropy ( $\Delta S$ ). According to the laws of thermodynamics, if the process is spontaneous (and it is) then the free energy is negative because the combination of  $\Delta H-T\Delta S$  is negative. If the process is not exothermic (i.e., not enthalpically driven) then it is entropically driven and so  $T\Delta S$  must be positive. That is to say, the process of adsorption of the surfactant molecule to the oil-water interface is one whose final state is more disordered than the initial state (bulk).

This seems strange; however, it can be explained. Kanicky is describing the situation of adsorption of the surfactant to the oil-water interface, so how is that specific process entropically driven? In the bulk phase of the oil, there might be some structure associated with the net repulsion of the hydrophobic part of the surfactant molecule. At the interface, Kanicky describes that if the hydrophobic tail is pointing into the oil layer and the hydrophilic head is directed into the water layer then, as a whole, the surfactant is thermodynamically stable, i.e. a minimum in free energy and maximum in entropy.

Recently there has been speculation that unwanted surface films can form in test facilities (Nedwed & Coolbaugh, 2008). It is proposed that the presence of these unwanted surface films interferes with the controlled testing of the dispersants and consequently underestimates the dispersant effectiveness test results. Crude oil naturally contains organic acids that are surface active agents or surfactant molecules and after addition of the crude oil to water; those surfactants will naturally form an interfacial film at the oil-water interface. The issue is the potential for surface films to form from oil and oil/dispersant applications through the process of molecular diffusion of oil and dispersant overspray.

There are a number of procedures to investigate the efficiency of a dispersant to act on an oil spill such as a visually inspecting the surface, testing/monitoring the hydrocarbon levels in the water phase and a Laser *In-Situ* Scattering Transmissometry (LISST 100x) for oil particle size distribution and volume concentration (Li, et al., 2008a). However; many evaluation procedures incorporate chemical and, to a lesser extent, physical measurements when conducting wave tank studies on chemically dispersed oil, which do not provide sufficient information to address the speculation of

the presence of surface film contamination of seawater during oil and oil/dispersant application.

The surface excess concentration ( $\Gamma$ ) is the difference between the solute concentration in the bulk and that at the interface. (Kanicky et al., 2001) The later is related to surface and interfacial tension according to Gibbs Adsorption equation (1-1). The  $\Gamma$  is related to surface and interfacial tension according to Gibbs Adsorption equation:

$$\Gamma = -\frac{1}{2RT} \frac{d\gamma}{d \ln C_{surf}} \quad (1-1)$$

where R is the universal gas constant, T is temperature (in Kelvin),  $\gamma$  the surface tension or  $\sigma$  for interfacial tension, and C the bulk concentration of surface-active species. The surface tension of seawater is the property of a liquid that permits it to resist to an external force (Kanicky et al 2001). Surface and interfacial tension are measured using a tensiometer, i.e. DuNouy ring. The cohesive (intermolecular) forces such as hydrogen bonding, Van der Waals and London Dispersion between seawater molecules are responsible for the surface tension of seawater. Interfacial tension is somewhat similar to surface tension where cohesive forces are involved. However, the main forces involved in interfacial tension are adhesive forces between the liquid phase of one substance and the liquid phase of another substance, i.e. at the oil-seawater interface. Therefore surface tension measurements of the test seawater can be used to assess the presence of any unwanted surface films in the test seawater.

### ***1.1 Objectives***

1. Investigate the rate of surface film formation during oil/oil dispersant application

to seawater in a static lab basin environment using interfacial tension measurements.

2. Determine if the effects of surface tension gradients (surface films) on seawater affect oil spreading rate in a lab basin.
3. Determine if unwanted interfacial films from oil and oil dispersant overspray applied to seawater affect oil dispersant effectiveness tests in a dynamic wave tank facility using interfacial tension measurements.

## **Chapter 2**

### **Literature Review**

#### ***2.1 Importance of Dispersants***

Oil and water are immiscible. Dispersant such as Corexit 9500 is commonly used though-out Canada, the United States, Norway, Australia and other nations to remediate accidental oil spills at sea (Nalco, 2010). Corexit 9500 is not a single compound, but is a mixture and contains ingredients such as dioctyl sodium sulfosuccinate; petroleum distillates, hydrotreated light; sorbitan derivatives; and propanol (Nalco, 2010). The salt is considered the primary surface active ingredient. Its hydrophilic (water loving) head interacts with the polar (water) phase and its hydrophobic (water repelling) tail interacts with the non-polar (oil) phase. The other additives (petroleum distillates) act as a vehicle that permits the dispersant to be applied to oil on seawater. The process is like dish washing soap that breaks apart oil and water in a kitchen sink.

When dispersants are applied to oil spills on seawater they interact with both oil and seawater requiring minimal energy to disperse the oil into small spherical droplets

(<70µm) into the seawater phase (Li et al., 2008a). The surface of the oil droplets coated with dispersant are transported by waves and current; therefore no coalescence in an open environment. Dispersants are applied at sea to remediate an oil spill and prevent the oil from approaching coastal areas where extensive damage can occur. Biodegradation is the natural process by which bacteria breakdown crude oil. Chemical dispersants have proven to be very effective in assisting and increasing the rate at which bacteria can biodegrade oil in seawater (Lindstrom & Braddock, 2002; Venosa & Holder, 2007). Biodegradation of crude oil can occur at low temperatures (e.g. 5 °C); however, at this temperature it is relatively slow. At low temperatures, the rate of evaporation is also slow for volatile components present in crude oil. The volatile components (benzene, toluene, ethylbenzene, and xylenes) act as an inhibitor to oil-degrading micro-organisms (Atlas and Bartha, 1972). Dispersants have been employed in lab mesocosms (experimental water enclosure) to promote carbon bioavailability of sediments contaminated with hydrocarbons and thus enhance biodegradation of petroleum hydrocarbons (Flaming et al., 2003).

Offshore oil and gas development has greatly increased over the past several years in Nova Scotia. This has resulted in increased ship traffic, drilling operations and effluent waste from oil and gas exploration; therefore there is a greater risk of oil contamination at sea. This risk has stimulated a growing interest by both industry and government in the use of chemical dispersants to remediate accidental oil spills at sea.

## ***2.2 Dispersant-Effectiveness Tests***

There are inexpensive flask test methods (e.g. swirling and baffle flasks) used in the laboratory to screen different dispersants for dispersant effectiveness on spilled oil

(Venosa et al., 2002). Different physical properties, such as temperature and salinity and chemical levels of the treated seawater in a standard flask test can be analyzed at depths below the seawater surface and over different time periods following the application event, to determine the extent and rate of surface oil break-up. There are questions, however, about uncertainties surrounding the control of all variables and therefore reliability of results and there is a need to be able to extrapolate the results of these small-scale tests to real-world applications is driving the development of better protocols (Singer et al., 2004; Venosa et al., 2002). Therefore, these procedures are considered in the scientific community as valuable screening techniques to determine the dispersant effectiveness on spilled oil prior to large-scale testing.

The Bedford Institute of Oceanography (BIO) in Dartmouth, Canada has designed and built a field mesocosm for dispersant effectiveness testing on oil spills. The dimensions of the wave tank are 0.6 meters in width, and 32 m in length with a depth of 2 m (Figure 2-1). The system is capable of generating transverse waves, spilling breakers, and plunging breakers (Figure 2-2). The system is calibrated to simulate natural conditions. The facility has been used to test the effectiveness of various dispersants on a wide range of crude oils under these various wave conditions (Li, et al., 2008b; Li et al., 2009). However, two questions have been raised: 1) does resurfacing of oil due to coalescence occur once the wave energy terminates and 2) does the closed system design address how dispersed oil is transported at sea?

To address the problems of coalescence of oil and dispersed oil transport, the wave tank facility has been modified to incorporate a flow-through (open) system (Figure 2-3). Seawater enters the front (wave paddle side) at a rate of 65 gallons/min through a

series of ½ inch valves on both sides of the tank and seawater leaves at the same rate through a similar valve system at the back end of the tank to a disposal tank that removes oil and returns clean seawater (Li et al, 2009). The open system has been calibrated by engineers to simulate natural sea current conditions in the wave tank facility. The facility is used in open mode to test dispersant effectiveness on spilled oil and the transport of dispersed oil under three wave conditions: transverse waves, spilling and plunging breakers. Sample ports are located at known locations and known depths in the tank. They are used to remove aliquots of liquid for different tests which can include tests for such properties as solute concentration, surface tension and fluorescence measurements. Typically, the properties measured to determine the effectiveness of an applied dispersant to a controlled oil slick in the test tank are: temperature, salinity, hydrocarbon concentrations, and real-time average-sized particle distribution and volume concentration.

Temperature and salinity are recorded using a portable handheld meter. The probe of the meter is submerged into the seawater of the tank. Once the readings are constant then temperature and salinity are recorded. When performing kinetic investigations of oil dispersant effectiveness it's essential to ensure these parameters are constant during the testing.

According to the Gibb's Adsorption equation (1), the slope is a constant under isothermal conditions and the surface excess concentration of the surfactant is equal to the value of the slope divided by the product of  $2RT$ . The result is essentially the difference between the concentration of the surfactant in the bulk and that at the interface, given in units of moles of surfactant per unit area. However, surface tension

measurements of seawater and interfacial tension measurements of oil-seawater interface and dispersed oil in seawater permits assessment of unwanted surface films that interfere in the evaluation of oil dispersant efficiency.

Another approach to assess dispersant effectiveness on spilled oil in open and closed systems is to measure the hydrocarbon levels at various depths in the water column of a wave tank following dispersant application. These methods involve a standardized sample collection, preservation, extraction and analysis of extracts by either infrared spectrophotometry or gas chromatography with flame ionization detection (Cole et al., 2007; Li et al., 2008b; Li et al., 2009). Briefly, the samples are extracted with dichloromethane on a roller apparatus for 18 hours. The solvent phase is separated from the seawater phase. Standards of the crude oil used in the study are prepared in the same organic solvent. The standards are analysed by gas chromatography coupled with flame ionization detection to generate a standard calibration curve. The sample extracts are analysed and hydrocarbon levels are generated. The results from the various tests are used to evaluate oil dispersant effectiveness on spilled oil in the wave tank.

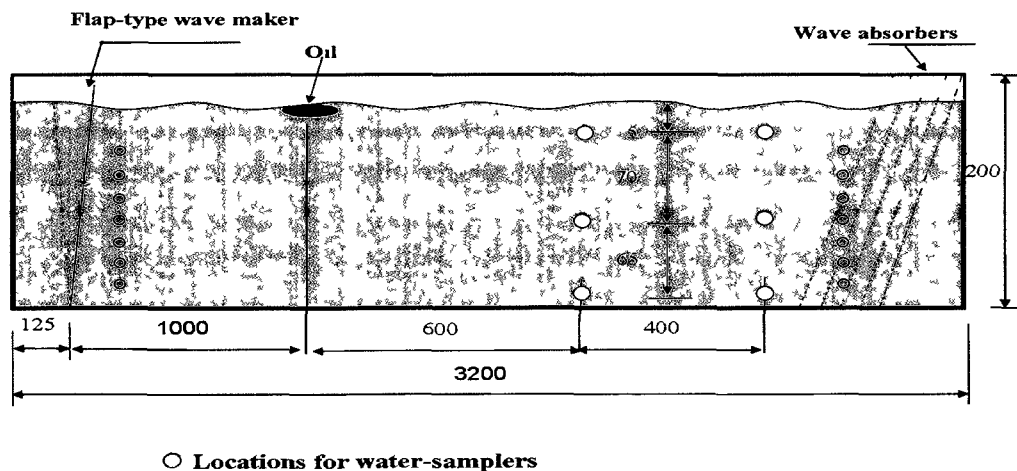


**Figure 2-1:** Schematic diagram of the wave tank (all units are in cm).



**Figure 2-2:** Photographs of the wave tank showing the different types of waves generated: A) transverse B) spilling breakers and C) plunging breakers

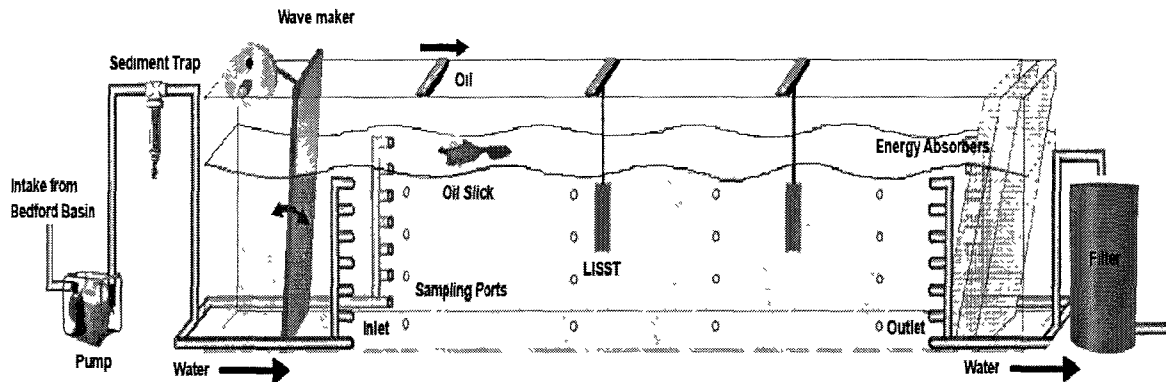


**Figure 2-3:** Schematic representation of the wave tank flow-through system (not to scale).

### ***2.3 Factors Affecting Dispersant Effectiveness***

The toxicity effects of oil dispersant applications on marine life are certainly a factor that can either reduce or eliminate its use to remediate oil spills at sea. There are studies that illustrate that dispersants, such as Corexit 9500, Corexit 9527, Corexit 9554, Slik-A-Way, Nokomis 3, and Corexit 7664, at high concentrations, e.g. 200 to 300 ppm, are toxic to fish (Singer et al., 1996). However, the concentrations used in these studies are 10 to 100 times greater than wave tank studies and real oil spill scenarios. Therefore, they do not provide a natural model of fish exposure to toxicants in dispersed oil. Other studies revealed that dispersant used on contaminated water containing chemicals of

different structures and lipophilicities did not affect the bioconcentration factors of these chemicals in Carp (Yakata et al., 2006).

Dispersant can be chemically formulated to be used in a specific environment, such as seawater. Dispersant effectiveness to remediate spilled oil at sea depends on a number of physical factors such as, oil properties, wave-mixing energy, temperature, oil weathering, and salinity of the sea water (Chandrasekar et al., 2006). Dispersants, such as Corexit 9500 are effective on oil slicks at various salinity levels; however, are more effective in water containing salinity greater than 25 ppt (Blondina et al., 1999). Some research indicates that dispersant effectiveness decreases with decreasing pH (Allered & Brown 2001). Other researchers have revealed that temperature affects dispersant effectiveness on spilled oil, notable as the water temperature increases it can shorten the time needed for the dynamic interfacial tension to reach steady-state (Vargaftik et al., 1983; Ye et al., 2008). Therefore, the dispersants used to remediate an oil spill at sea are considered to be more effective in warmer water. Oil weathering (evaporation) can affect dispersant effectiveness as well; however most researchers, in order to eliminate this problem, artificially weather crude oil prior to use. In recent studies, Nedwed and Coolbaugh demonstrated the effects of a surface film on oil spreading, thus generating thick oil slicks (2008). Thicker oil slicks require greater energy to disperse the oil into the seawater.

Variables such as pH, salinity, temperatures, oil weathering and surface films can either positively or negatively affect dispersant effectiveness depending on the conditions. The first three have been extensively studied in small scale microcosms in the lab as illustrated in this literature review. However, limited information is available in the

literature on unwanted surface films formed during oil/oil dispersant applications and their effects on oil spreading rate and dispersant effectiveness tests in wave tanks.

#### ***2.4 Recommended Research and Potential Problems***

A surface film may be generated under static conditions when crude oil is introduced to seawater (Kanicky et al., 2001). Crude oil contains surface agents in the form of resins and asphaltenes, which are the polar constituents of the oil (Abdurahman & Yunus 2009). The oil upon contact with the water surface releases these surface agents which reduce the interfacial tension of the seawater and induce repulsive forces that can restrict the spreading of oil in confined boundaries. In addition, chemical dispersants such as Corexit 9500 may be applied to the oil under these conditions and further contribute, by overspray, to the induced repulsive forces resulting in thicker oil lens. This generates a condition in test systems (wave tanks) which may underestimate the dispersant effectiveness tests.

Fay proposed a model for the spreading of oil slicks under static sea conditions. The spreading coefficient ( $\sigma_s$ , dynes/cm)  $= \gamma_{aw} - \gamma_{ao} - \gamma_{ow}$ ; where,  $\gamma_{aw}$  is air-water surface tension,  $\gamma_{ao}$  is air-oil surface tension, and  $\gamma_{ow}$  is oil-water interfacial tension (Fay, 1969). According to Fay, once the oil passes the gravity-dominated spreading phase, if the spreading coefficient is positive, then oil spreads freely to form a thin film. If the value is negative then oil tends to form a thicker lens on the water surface. Thicker oil slicks require more physical energy to disperse.

Nedwed and Coolbaugh demonstrated in lab basin tests, the effects of unwanted surface films (surfactant) on oil spreading coefficients (2008). Speculation that a surface film is generated during oil spill and dispersant applications raised concern about

evaluating dispersant effectiveness tests in large-scale mesocosms, such as wave tanks. However; the basin studies conducted by Nedwed and Coolbaugh was based on Fay's model which did not provide a direct measurement of the oil spreading rate, although it can be applied to predict whether spreading will occur on seawater (Hale & Mitchell, 1997). Others revealed that as the surfactant concentration increased in the water column the breaking (spilling) waves decreased in amplitude and number, the size of the bulge shrinks, and the ripples diminish (Liu & Duncan, 2003). All of which can introduce unnatural sea conditions during dispersant-effectiveness testing. This issue of surface films is confined to test systems that have boundaries (walls). Surface films naturally occur at sea or as the result of overspray of dispersant on accidental oil spills; however, films in the open environment are believed to be very fragile, thus not posing a problem since there are no boundaries to consider that enhance film build-up (Nedwed & Coolbaugh, 2008).

Essential information is not available on how surface films affect oil dispersant effectiveness test in large-scale systems, such as wave tank in terms of oil spill and dispersant applications. Kinetic investigations have not been performed to address the effects of unwanted surface films (surfactants) on oil spreading rates. The effect of unwanted surface films on dispersant effectiveness tests has not been assessed in the wave tank at Bedford Institute of Oceanography.

### ***2.5 Research Questions/Recommendations***

The following questions are proposed with recommendations to address the issue of unwanted surface films (surfactants) formed during oil/oil dispersant applications to seawater in oil dispersant test systems.

### ***2.5.1 Will Surface Films Form During Oil/Oil Dispersant Application to Seawater in a Static Environment?***

Surface agents (resins/asphaltenes; polar phase containing fatty acids and other constituents) are naturally present in crude oil. Crude oil chemical composition can be characterized using thin-layer chromatography followed by scanning flame ionization detection (Dutta & Harayama, 2001; Maki & Sasaki, 1997). Oil standards are applied to silica gel rods. The rods are developed in a series of chromatographic tanks filled with solvents of different polarities. This allows the oil to be partitioned into four main classes: saturates, aromatics, resins, and asphaltenes (SARA). The rods are then placed in a scanning flame ionization detector (IATROSCAN) to provide semi-quantitative values for the SARAs (Maki & Saki, 1997).

Surface films can be generated in oil dispersant test systems. A known quantity of oil is applied to an open containment barrier on the surface of seawater and the physical property measurements (e.g., surface tension and viscosity) of the surrounding water phase can be made over time. Likewise, dispersant can be applied to the oil phase and physical measurements continued to determine surface film contribution from dispersed oil and dispersant overspray, respectively. The concept, on a smaller, cheaper scale, would permit the determination of surface film formation in wave tank seawater during oil and oil/dispersant applications.

### ***2.5.2 What Effect Do Surface Films on the Seawater Surface Have on the Oil Spreading Rate in a Static Environment?***

Surface films can be quantitatively produced and, through interfacial tension

measurements, be monitored until a steady-state in dynamic interfacial tension is achieved (Saylor, 2003). A kinetic investigation could be conducted to determine the effect on the oil spreading rate on seawater in the presence of surface films (surfactants). As a first approximation, the radial rate of oil spreading on the surface of the water is assumed to be equal in all radial surface directions and thus can be taken as being equal to the rate of thinning of the oil. This rate of thinning is also assumed to follow first-order kinetics. Thus, the oil film thickness at any time is expressed as ( $h_t$ ) but is equal to the difference between the height at that time ( $h$ ) and the terminal height value achieved at the end of spreading ( $h_{\infty}$ ). With the spreading coefficient expressed as  $\gamma$  the spreading rate of oil on the water surface can be taken as equal to the rate of oil thinning,  $dh_t/dt$ . Thus:

$$\gamma = \frac{dh_t}{dt} = -k(h_t) \quad (2-1)$$

The  $k$  is the first order rate constant and has reciprocal time units. An integrated rate law expression can be derived by integrating the above expression between the limits of thickness of initial thickness,  $h_{t_0}$  to the thickness at any time,  $h_t$  and; between the limits of initial time,  $t_0$  and any time,  $t$ :

$$\int_{h_t}^{h_{t_0}} \frac{dh_t}{h_t} = - \int_{t_0}^t k dt \quad (2-2)$$

The integration is solved as:

$$\ln(h_t) = \ln(h_0) - k(t - t_0) \quad (2-3)$$

The initial time is taken to be equal to zero so that  $(t - t_0) = t$ . The solution can be rearranged to give:

$$\ln(h_t) = \ln(h_0) - kt \quad (2-4)$$

Upon rearrangement the solution expresses the integrated rate law as an equation of a line,  $y = mx + b$ , so that a plot of the natural logarithm of thickness against time should yield a straight line with the first-order reaction rate constant as the negative value of the slope. The line thus predicts the value of the oil film thickness at any time *not* in the time period approaching the terminal thickness. Comparing  $k$  values for oil spreading on clean and contaminated (surface film) seawater will aid to quantitatively determine the effects that a surface film has on oil spreading. The reaction rate constant is constant so long as there is no catalytic effect and/or temperature change. The value of  $k$  depends on temperature, therefore the oil spreading experiments are carried out under isothermal conditions (20 °C). A good fit of the data to a straight line supports the idea that the spreading rate is indeed first-order. However, if the slope is not constant, that is, if the data does not fit well to a straight line, then the spreading is not a first-order process.

This study will employ containment of the oil in a closed barrier prior to release to ensure that there are no residual surface agent effects from the oil. There are a number of kinetic studies using high speed video for measuring bacteria spreading rates in the presence of a monolayer and kinetics on low viscosity oils that can be adapted to provide direct measurements of oil spreading with/without a surface film in a closed system (Drelich and Miller, 2000).

The results from the investigations of surface films formations from oil/oil dispersant applications and the effect of surface films on oil spreading rate will be compared to those corresponding results from the study by Nedwed and Coolbaugh to determine whether unwanted surface films (surfactants) will significantly affect dispersant effectiveness tests in a closed system (wave tank).

### ***2.5.3 What Affect Do Surface Films (Contaminated Seawater) Have on the Oil Dispersant Effectiveness Tests in a Dynamic Wave Tank?***

A preliminary investigation of the effects of dispersed oil on the interfacial tension of seawater in the BIO wave tank facility has indicated that the interfacial tension (non-steady state) can be used to assess the effect of compounding factors and their collective effects are difficult to deconvolute in order to attribute effects to individual factors such as temperature and most probably a surface film on the dispersant-effectiveness (King et al., 2010).

In the current work, the proposed bias imposed by an interfering or unwanted surface film on oil spreading is quantified by the measured difference in interfacial tension between dispersed oil in clean and contaminated (surface film) seawater under the following conditions:

1. oil and dispersant under breaking wave conditions;
2. oil and dispersant in the presence of surfactant monolayer under breaking wave conditions;
3. oil with no dispersant under breaking wave conditions (natural attenuation).

Surface and interfacial tension and hydrocarbon levels are required to assess the impact of unwanted surface films on oil dispersant effectiveness tests. Total hydrocarbon measurements will help to track the oil levels in the water over time. The hydrocarbon levels will complement the physical measurements. The methods used were briefly described in section 2.2.

## **Chapter 3**

### **Experimental Description**

### ***3.1 Oil Characterization and Dispersant Information***

The test oils used in the study were Arabian Light Crude (ALC, artificially weathered by aeration to 93% by volume to remove volatiles), Alaskan North Slope Crude Oil (ANS, artificially weathered by aeration to 90% by volume to remove volatiles), and Intermediate Fuel Oil 120 (IFO 120). All oils were characterized using thin-layer chromatography followed by scanning flame ionization detection IATROSCAN MK6 (Shell, USA) (Maki & Sasaki 1997). Oil standards of known concentrations were prepared and spotted on silica gel rods (thin-layer chromatography IATROSCAN rods). Once the rods were spotted they were developed using the following conditions:

- H<sub>2</sub>SO<sub>4</sub> (Sulfuric acid, Drying chamber) – 10 minutes
- Hexane – 25 minutes
- H<sub>2</sub>SO<sub>4</sub> – 10 minutes
- Toluene – 15 minutes
- H<sub>2</sub>SO<sub>4</sub> – 10 minutes
- 95:5 Dichloromethane:methanol (DCM:MeOH) – 5 minutes

After each development stage the silica rods were allowed to air dry for 2 minutes before moving onto the next stage. This process permitted the oils to be separated into their four main classes, namely SARAs. The semi-quantitative determination of SARAs was achieved using the IATROSCAN in flame ionization mode.

The viscosities of the oils at desired temperatures were determined using a LV Dial-Reading Viscometer (Brookfield, Canada) and their densities ( $\rho$ =mass/volume) calculated by determining the mass of a determined volume of the oil.

Corexit 9500 (Nalco Energy Service, L.P. Sugar Land, TX), a commercially available product frequently stockpiled for use by oil spill response agencies in Canada and the United States, was used as the reference oil dispersant. The density of Corexit 9500 is 0.948 g/mL.

### ***3.2 Adsorbed Film Formation (Basin Tests)***

A lab basin ( $1\text{ m}^2 \times 0.15\text{ m}$  high) was constructed from 6.4 mm thick standard acrylic with the aid of the engineering group at the Bedford Institute of Oceanography (Figure 3-1). The lab basin was filled with filtered ( $25\ \mu\text{m}$ ) seawater (20 L), obtained from the BIO aquarium, to achieve a water depth of 2.54 cm, which is an ideal surface area for horizontal interfacial tension gradient formation. Oil (quantitative to achieve a thickness of 2.40 mm, similar to wave tank studies) was applied and contained in an open oil containment barrier (spliced tubing 9.0 cm i.d.). Dynamic interfacial tension ( $\gamma$ ) and viscosity ( $\eta$ ) measurements were taken from samples (50 ml of surface at 10 cm from oil containment barrier) of the water phase surrounding the barrier, over time (0, 10, 30, 60, 120, 180 and 240 minutes) until the surface agents diffusing from the oil to the water produced constant interfacial tension values. The viscometer was equipped with a UL adapter (Fisher Scientific, Canada) operated at a speed of 60 revolutions per minute with a shear rate of  $73.38\ \text{s}^{-1}$ . Replicate analyses ( $n=3$ ) were performed in a laboratory basin using three oils: ALC, ANS, and IFO 120. The procedure was repeated in replication using all oils with dispersant application. This process was repeated with ALC using a closed oil containment barrier (3 inch ABS Coupling 9.0 cm i.d.; Kent Building Supplies Ltd., Dartmouth N.S. Canada) over the same time series. However, since it is a closed

barrier, oil is restricted from entering the surrounding water phase and this concept provided an adequate control for the study.

The basin was cleaned between experimental trials by removing all surface oil with adsorbent pads (Zep, Canada) and draining the waste water into a 20 L Nalgene container. The tank was wiped free of oil using 'Big Orange' hand towels (Zep, Canada) and rinsed several times with clean distilled water. The entire surface area was dried using commercial paper towels. Once dry, the tank was wiped with paper towel dipped into a small quantity of hexane (ACS specifications, Caledon Labs, Canada) to ensure all traces of oil were removed. The tank was filled with clean seawater and surface tension measurements were taken. The surface tension of clean seawater was  $\sim 74$  dynes/cm, this value ensure cleanliness (no surfactants) after cleaning.

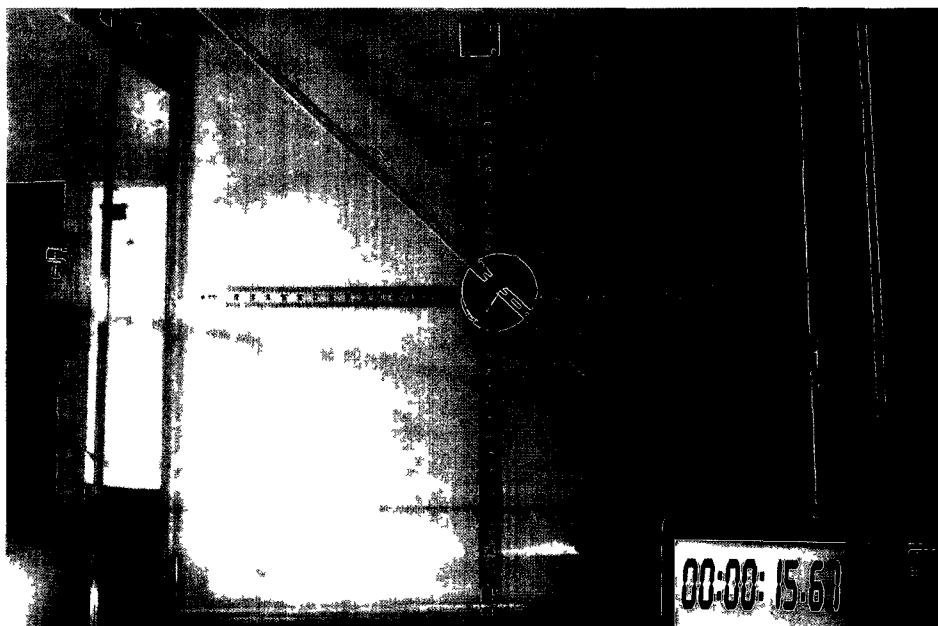


**Figure 3-1:** A photo of the lab basin used for diffusion and oil spreading studies.

### ***3.3 Kinetic Investigations of Oil Spreading***

The same test basin in Chapter 3.2 was used for the kinetic investigations of oil spreading on seawater (Figure 3-1). The closed oil containment barrier was used, which was suspended by fishing line (3 lb test, Crystal River, Reno, NV USA) and controlled by a fishing reel (Quantum, Zebco Precision Engineered, Tulsa, OK USA), supported by a 6.4 mm wide by 1.1m long perforated steel bar. This apparatus provided gentle and constant control of the oil containment barrier, which ensured a symmetrical oil lens and that the simulated surface films remained intact when releasing the oil. A Canon Rebel T1i (Canon EF 10-20 mm lens) capable of both video (1080p, 20fps) and continuous drive modes (8Mp, 3.7fps) was suspended by a camera stand above the lab basin. The camera was set at an area shutter speed of 1/100 seconds, aperture of f/5.6, ISO of 800 and focal length of 15 mm. A scale was created in both vertical and horizontal directions at the bottom of the lab basin (Figure 4). Since acrylic is clear this was achieved by taping a one meter adhesive backed ruler (ER-S036L-TC; Oregon Rule Co., Oregon USA) to the underside of the basin. A Panasonic laptop (Panasonic AVC Networks, Taiwan Co. Ltd, Taiwan) was used to produce a large display stopwatch and in some cases control the camera.

The oil was quantitatively added to achieve an initial thickness of 2.4 mm at time zero seconds (s) inside the oil containment barrier. The containment barrier was raised by using the fishing reel. The oil was released and either video or continuous drive mode recorded the evidence of oil spreading on seawater over time. For the surface film effects on oil spreading trials, a surface film on the seawater surface was generated by placing 1 drop ( $7.64 \pm 0.17$  mg or  $\sim 0.008$  mL/m<sup>2</sup>) of Corexit 9500 from a calibrated Pipetplus (LTS 20, J02022100, Rainin, USA) set at 19.0  $\mu$ L. Due to the viscosity of the Corexit 9500 not

all the surfactant was dispensed from the pipette; therefore it was calibrated by determining the mass of a dispersant droplet. The surface film generated, based on testing, was sufficient to slow oil spreading so that it could be studied within a reasonable time (a few hours).

Two oils, ANS and IFO 120, were tested to investigate oil spreading on seawater with/without surface film interference. The tests were replicated to ensure accuracy and precision of measurements. The initial oil thickness was determined by treating the oil containment barrier as a cylinder. The volume of a cylinder is expressed as (3-1):

$$V = \pi r^2 h_o \quad (3-1)$$

where  $V$  is the volume of oil,  $r$  is the radius (i.d.) of the oil containment barrier, and  $h_o$  is the initial oil height taken as proportional to oil thickness. The initial volume and radius are known so the equation can be rearranged to calculate initial oil thickness ( $h_o$ ). Oil thickness ( $h_t$ ) was generated using the same concept, since the oil while spreading maintained its original shape (Appendix B, Example Calculation 1). The diameter of the oil containment barrier was 9.0 cm (i.d). The initial lens measurement was taken from the center to the outer edge of the lens, which was 4.5 cm (45 mm). The pictures generated from the study were analysed and the average radial distance of the oil lens growth in two directions was recorded at various time (s) intervals. All measurements were taken in inches and converted to metric units. Between trials the basin was cleaned as outlined in Chapter 3.2.

### ***3.4 Surface Film Impacts on Dispersant Effectiveness (Wave Tank)***

This study involved using one oil (ANS), which was dispersed using three

different treatments: A) natural attenuation (no dispersant or created surface film); B) chemical dispersant (no surface film); and C) surface film (with dispersant use).

Treatment A represents a natural control and provides information on whether a surface film forms during oil application to wave tank seawater and if they do what are the effects on natural, physical dispersion of oil. Treatment B represents normal operations when oil is chemically dispersed in wave tank seawater. Treatment C represents a surface film that is created to understand the effects of dispersant overspray on oil dispersant effectiveness in wave tank seawater under dynamic conditions. The factorial design was performed in triplicate and in random order to reduce the effects from temperature, salinity and wind.

### ***3.41 Wave Tank Operations***

Figure 2-1 (Chapter 2.2) is a schematic diagram of the wave tank facility located at the Bedford Institute of Oceanography (Dartmouth, Nova Scotia, Canada). Filtered seawater was pumped (230V, 60Hz Electric Centrifuge Pump model#C184K34FK4A 5 HP, Leeson, Canada) from the Bedford Basin (Dartmouth, N.S., Canada) through filtered (two 5 µm inside a 25 µm) socks (Atlantic Purification Ltd., Dartmouth N.S., Canada) into the wave tank. The water depth was maintained, throughout the studies, at 1.5m (~29,000 litres of seawater). Temperature and salinity of the seawater (Salinity, Temperature and Conductivity meter, YSI model #30-1-FT; YSI Inc. Yellow Springs, Ohio, USA) were recorded prior to each experimental run. In addition, air temperature and weather conditions were recorded.

Waves were generated by a computer-controlled flap-type wave maker situated at one end of the tank linked to an adjusted cam that controlled stroke length in order to

alter wave-height characteristics (Li et al., 2008b). As per Li et al., (2009), plunging breaking waves were produced with a 12 cm stroke and alternating trains of high-frequency waves (0.85 Hz, wave length 2.16 m, wave height 26 cm, and duration 20 s). Plunging breaker waves are similar to white caps generated in ocean seawater during a windy day, when the crest of the wave breaks it appears white in color.

Two samplers were employed downstream, one at 6m and the second at 10m, from oil release. Oil was released 10m downstream of the wave maker. Each sampler collected water (120 mL) at three depths (5, 75 and 145 cm) from the tank. Samples were collected at time points of 5, 15, 30, 45, 60, 75, and 90 min. A time zero was randomly taken from one sampler location throughout the study.

#### ***3.42 Natural Attenuation of Oil and Oil Treated with Dispersant***

For each experimental run, oil was quantitatively released in a (40 cm inside diameter) containment ring (constructed of NSF-51 reinforced clear PVC tubing) located 10 m downstream from the wave maker. In the case of chemically dispersed oil, dispersant (12 mL; container massed prior to an after) was sprayed onto the surface of the oil slick through a pressurized (~30 psi; 0.635 mm i.d.) calibrated spray nozzle. This resulted in a dispersant-to-oil ratio (DOR) of ~1:25. No dispersant was used for natural attenuation of oil. The ring was then lifted prior to the approaches of the first wave, which occurred several seconds after the start of the wave generator.

#### ***3.43 Created Surface Film and Chemical Dispersion of Oil***

The seawater surface monolayer is defined as the upper layer of the water phase and it has a thickness of <1.0mm (Stolle et al., 2010). Any surface film produced would

be in the upper layer of the water phase. Under normal operations the contained oil and dispersant are not released until the approach of the first wave. In order to determine the effects dispersant overspray has on oil dispersant effectiveness in wave tank seawater, the surface film generated from overspray must come into contact with the applied oil and dispersant. Since it is difficult to control dispersant overspray, the procedure outlined below provided a controlled environment for the created surface film to come into contact with the applied oil and dispersant. A surface film was generated by adding 50 g of Corexit EC9500A using a 50 mL gas tight syringe (Hamilton, USA) to the seawater surface inside the oil containment ring. The dispersant was added drop-wise, based on surface film formation studies conducted by Nedwed & Coolbaugh (2008). This is illustrated in Figure 3-2. This technique produced a surface film with an interfacial tension of  $31.3 \pm 0.17$  dynes/cm inside the containment ring.

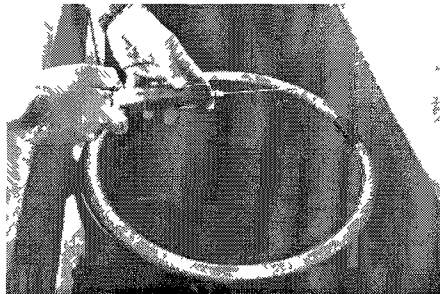


**Figure 3-2:** A photo of a created controlled surface film in the wave tank.

#### ***3.44 Lab Analysis of Disperse Oil Water Samples***

An aliquot (40 mL, using a 50 mL graduate cylinder) of each water sample from the wave tank studies was taken to measure either surface or interfacial tension using a Tensiomat 21 (Fisher Scientific, Canada) according to ASTM D971-99a (2002) in a temperature controlled environment ( $20.7 \pm 0.4$  °C). If samples were not immediately

analysed they were stored at 4 °C for no more than two days prior to measurements. No preservatives were added, since the addition of acid (6 N HCl) would introduce a bias into the interfacial tension measurements. For each sample, surface tension readings were taken several times until there were three readings within '1.0' dyne/cm. Average values and standard deviations were calculated.

The remaining wave tank sample volumes were determined by mass and 15 mL of dichloromethane (distilled in glass grade, Caledon Labs, Canada) was dispensed into each, followed by 30 seconds of shaking by hand. The samples were then placed on a Wheaton R<sub>2</sub>P Extraction Roller (VWR Scientific, USA) and extracted for 18 hours (Cole, King et al., 2007). Since no preservatives were added, all extractions were performed either immediately after wave tank runs or within a couple of days. This ensured that the sample integrity was not compromised by microbial degradation. After extraction, the solvent was removed with a 10 mL gas tight syringe (Hamilton, USA) and placed into a pre-weighed 15 mL centrifuge tube. The sample extracts were concentrated under nitrogen to the 1 mL graduation on the centrifuge tube. The samples were weighed and the mass of the extracts were determined by the difference between the empty tube and the tube with the sample extract. The final volume of the sample extract was determined by dividing the sample extract mass by the density of dichloromethane based on lab temperature (20 °C). An aliquot of the sample extract was placed into a gas chromatograph (GC) vial and capped. The vials were stored in a flammable storage refrigerator at 4 °C prior to analysis by GC coupled with flame ionization detection (FID). For total hydrocarbon analysis, a 1.00 microlitre (µL) aliquot of the extracted sample was injected into a 6890 GC (Agilent, Canada) equipped with a flame ionization

detector operated using the Agilent GC Chemstation software. The sample extracts were run on a MDN-5 capillary column (Supelco, Canada) using cool on-column injection in oven track mode. The GC conditions were as follows: initial oven temperature of 50 °C hold for 2.00 minutes ramp at 30 °C/minute to 300 °C hold for 10 minutes. The flame ionization detector is set at 320 °C with H<sub>2</sub> and air flows of 40 mL/min and 450 mL/min, respectively. A seven point calibration was generated using standards prepared from ANS oil. Total area under the curve is employed in each case. This semi-quantitative method is used for the determination of total petroleum hydrocarbons in extracts of seawater with a detection limit <1.0 mg/L.

## **Chapter 4**

### **Results and Discussion**

#### ***4.1 Oil Characterization***

The oils selected for this study have been previously evaluated in the wave tank. The oils were characterized prior to use and the data is presented in Table 4-1. IFO 120 is the more dense and viscous of the three oils analysed. The American Petroleum Institute gravity (API gravity) values indicate how light or heavy petroleum oil is compared to water. ALC, as its name implies is a light grade oil with an API gravity >31. ANS is medium grade oil (API gravity 22-31) and IFO 120 is similar to heavy oils (API gravity <22).

Thin-layer chromatography of crude oil followed by scanning FID permits crude oils to be separated into four main classes: alkanes, aromatics, resins and asphaltenes (SARA). The alkanes and aromatics are the low molecular weight non-polar fraction of crude oils. The resins and asphaltenes are generally defined as the high molecular weight

polar fraction of crude oils. The ratio of low to high molecular weight fractions provides information on how efficient oil dispersants may be on the various grades of crude oil. As in the case of heavy oils (more viscous) a higher dispersant to oil ratio (1:10) is recommended compared to a dispersant to oil ratio (1:25) for light and medium grade oils based on lab studies (Lunel & Lewis, 1999). The aromatic content provides beneficial information, since the aromatic fraction of the crude oil is considered to be toxic to marine life. The chemical and physical composition of each of the oils provides inferences on the fate and effects of dispersed oil in the marine environment.

**Table 4-1:** Physical and chemical compositions of oils used in the study.

Oil	Chemical Composition				Physical Composition		
	Alkanes	Aromatics	Resins	Asphaltenes	Weathered	$\rho$	$\eta$
	%	%	%	%	By vol.	20 °C	20 °C
	%	%	%	%	%	g/cm <sup>3</sup>	cP
ALC	32.7	18.9	46.9	1.5	7	0.8691	15.5
ANS	32.0	39.3	24.4	4.3	10	0.8607	17.5
IFO120	21.9	39.0	34.8	4.3		0.9469	117 (50°C)

#### ***4.2 Surface Tension Measurements and Instrument Calibration***

A Tensiomat 21 with a Du Noüy ring was used to record surface and interfacial tension measurements. The instrument was calibrated by preparing a series of standards (0.00, 0.50, 2.00, 2.50, 2.75, 3.00, 3.25, 5.00, 7.75, and 10.00 ppm) of Corexit 9500 in seawater and recording interfacial tensions for each at constant temperature (20 °C). The interfacial tension readings were plotted as a function of the natural logarithm of Corexit 9500 concentrations according to Gibbs Adsorption equation (Figure 4-1). Regression

analysis on the linear portion of the curve produced a coefficient of variance ( $r^2=0.98$ ,  $n=5$ ) and the ANOVA produced statistically significant  $p$ -value of 0.0016 with a standard error of 1.17. Oil standards in seawater were produced, but high concentrations ( $>25$  ppm) were needed to produce a small change in interfacial tension. Surface tension readings of distilled water ( $72.9 \pm 0.2$  dynes/cm,  $n=6$ ) were taken regularly and compared to a literature value of 72.8 dynes/cm at 20 °C (ASTM D971-99a, 2002). The equation of the line illustrated in Figure 4-1 demonstrates that the instrument is working according to theory. The concept of using interfacial tension measurements to provide temporal and spatial profiles of dispersed oil in a dynamic wave tank was demonstrated by King et al., 2010. The technique provides rapid assessment, where  $\sim 100$  samples could be measured in a regular eight hour working day. There is no preparation involved, since interfacial tension of the dispersed oil samples is directly read.

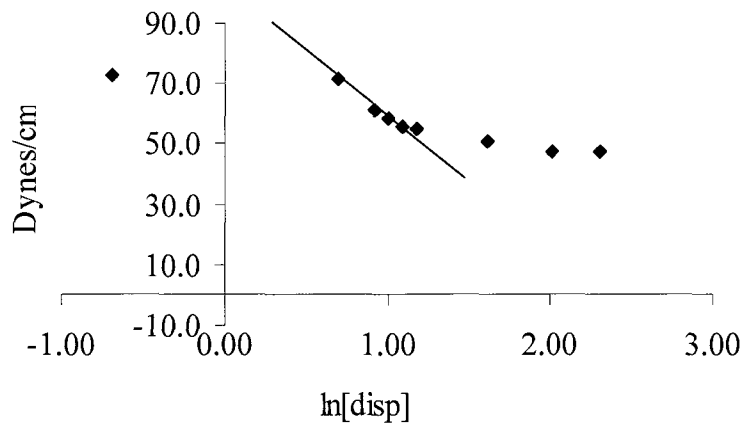


**Figure 4-1:** A plot of interfacial tension as a function of the natural logarithm of dispersant concentration.

#### ***4.3 Interfacial Tension Gradients Formed on Basin Seawater***

Interfacial tension and viscosity results for all three oils with and without

dispersant application over four hours are illustrated in Tables A1-A5 (Appendix A). The average results (n=3) are presented for the oils investigated. Figures 4-2 & 4-3 provide a graphical depiction of interfacial tension and viscosity of a newly created surface film over time. The rate of surface film formation from oil applied to basin seawater was rapid (10 minutes) as illustrated by a reduction in interfacial tension, which was evident for ALC and ANS. There was no evidence of surface film formation from the application of IFO 120 to basin seawater. The viscosity results were near background (clean seawater) for the oils except ALC.

Once dispersant was applied to oil the rate of surface film formation on the seawater surface increased. Viscosity results for the oil/dispersant application to seawater were similar for all oils except for a slight increase at 60 minute for ALC.

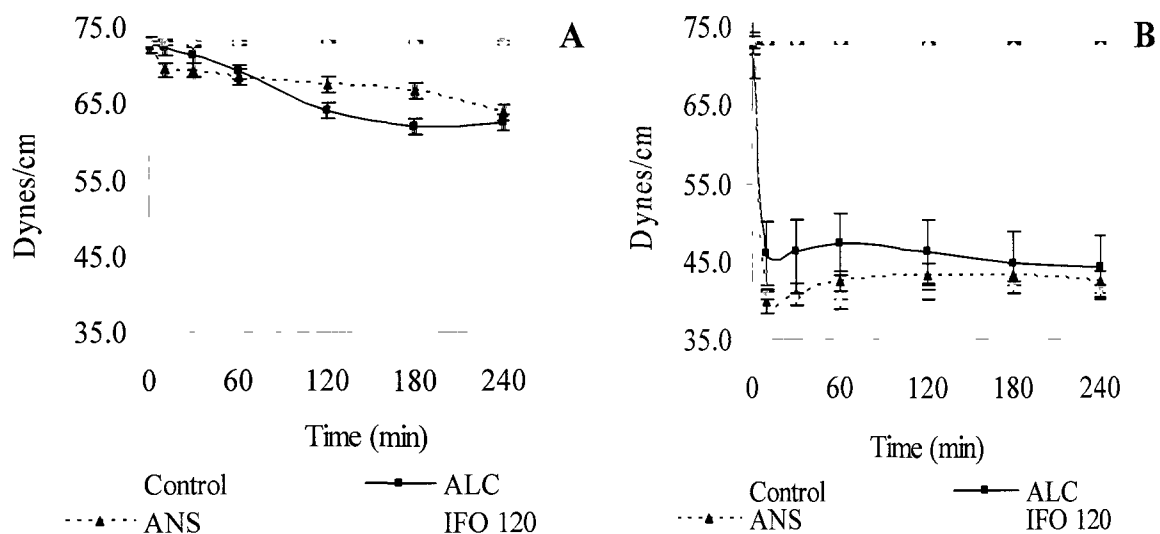


**Figure 4-2:** A plot of interfacial tension as a function of elapsed time indicating surface film formation from A) oil & B) oil/dispersant applied to basin seawater.

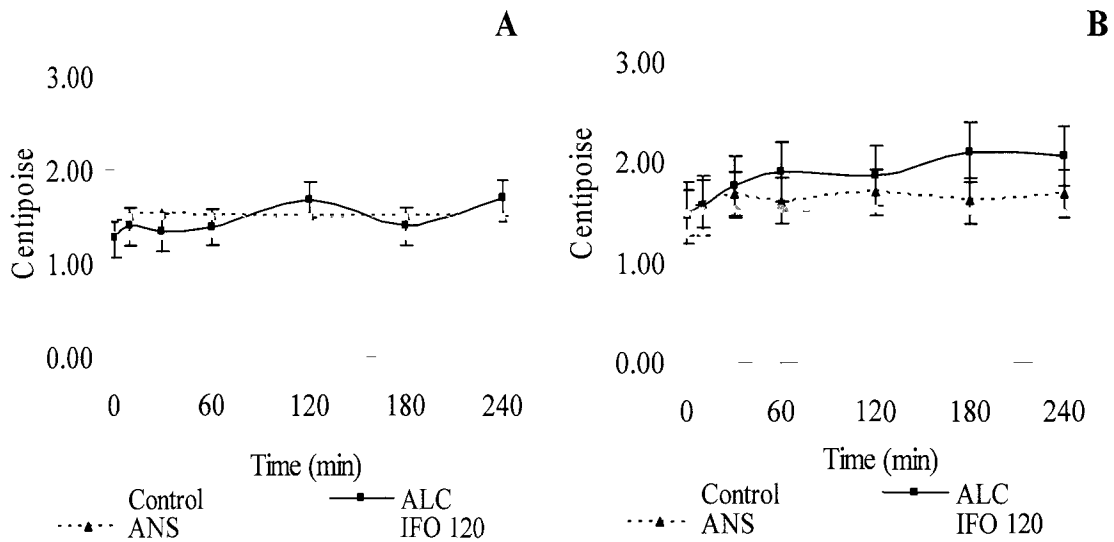


**Figure 4-3:** A plot of viscosity as a function of elapsed time A) oil & B) oil/dispersant applied to basin seawater.

Diffusion controlled short-time limit adsorption can be expressed by the following mathematical formula (4-1):

$$\gamma(t) = \gamma_0 - 2RTC_0 \sqrt{\frac{Dt}{\pi}} \quad (4-1)$$

where  $\gamma(t)$  and  $\gamma_0$  are either the surface (single liquid) or interfacial (two or more liquids) tension at time ( $t$ ) and initial surface tension (Dynes/cm or  $1.0 \times 10^{-5}$  Newtons/cm) respectively,  $R$  is the ideal gas constant,  $T$  is the temperature in  $^{\circ}\text{K}$ ,  $C_0$  is the surfactant concentration, and  $D$  is the diffusion coefficient. For short-time limit adsorption driven by diffusion, a linear relationship exists between  $\gamma(t)$  and  $\sqrt{t}$  which is illustrated in Figure 4-4. The slopes of the curves are  $-1.05 \times 10^{-6}$  and  $-6.08 \times 10^{-7} \text{ Ncm}^{-1}\text{s}^{-1/2}$  for ALC and ANS respectively. Regression analysis produced  $r^2$  values of 0.917 and 0.912 ( $n=7$ ) for ANS and ALC respectively. The results of the analysis of variance (ANOVA) using Microsoft Excel Data Analysis add-in produced statistically significant  $p$ -values of  $7.05 \times 10^{-4}$  and

$8.01 \times 10^{-4}$  and standard errors of 1.50 and 0.89 for ALC and ANS respectively. The  $p$ -values  $< 0.05$  rejects the null hypothesis that they are unrelated variables.

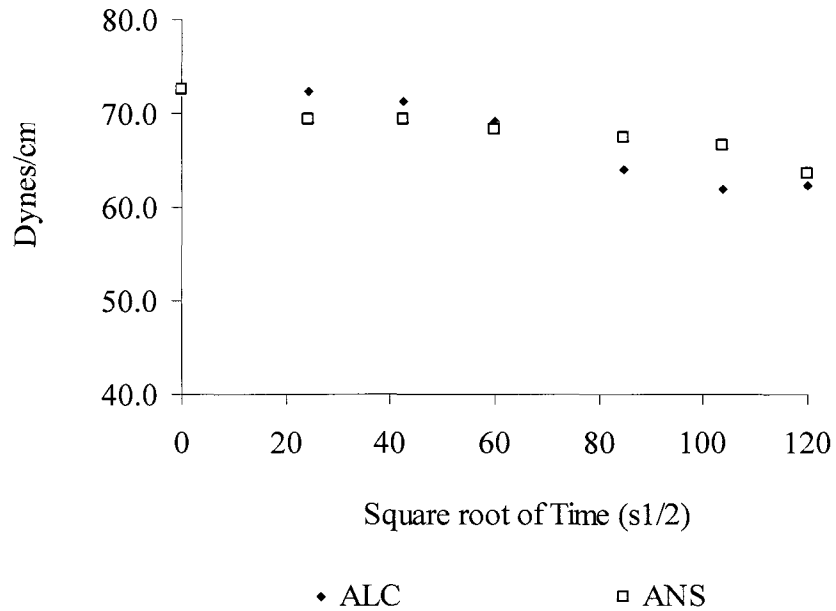


**Figure 4-4:** A plot of interfacial tension as a function of the square root of time ( $s^{1/2}$ ) for ALC & ANS.

The diffusion coefficient calculated from the slope of the curves was on the order of  $3.83 \times 10^{-6}$  and  $1.62 \times 10^{-7} \text{ cm}^2 \cdot \text{s}^{-1}$  considering the 1.5% & 4.3% (Table 4-1) of asphaltenes detected in ALS and ANS respectively (Appendix B, Example Calculation 2). Quintero et al. (2009) estimated a  $D$ -value on the order of  $10^{-9} \text{ cm}^2/\text{s}$  for crude oil. The  $D$  values determined in this study may be underestimated, since crude oil contains other polar constituents such as fatty acids that may contribute to surface film formation. Also, crude oils vary in chemical composition making it difficult to compare these values to those calculated by others in the literature. Temperature is another factor to take into consideration when determining  $D$ -values.

Interfacial tension measurements adequately provided temporal profiles of surface film formation from oil and oil/dispersant application to seawater over time under static conditions in a lab basin. The study on a miniature scale is an inexpensive way to determine if surface films form during oil and oil/dispersant applications to wave tank seawater. The potential for surface film build-up and formation in wave tanks under static conditions is likely to occur. This of course depends on the amount of oil used and whether oil dispersant overspray is controlled.

#### ***4.4 Interfacial Tension Gradient Effects on Oil Spreading Rate***

The average oil spreading results with/without surface film effects are presented in Tables A5 to A9 (Appendix A). The surface film was generated with Corexit 9500 to illustrate the effects that oil dispersant overspray has on oil spreading in a closed system. Three trials were performed for ANS and IFO 120 and duplicate trials for IFO 120 and ANS with surface film interference. Table A6 displays data for ANS spreading on seawater using the camera in continuous drive mode. The data compares very well with the results in Table A5, where the camera was used in video mode. All remaining oil spreading studies were documented using the camera in continuous drive mode, which was more than adequate and provided detailed images. In Tables A5-A9 in some cases a single data point is presented, because it was difficult to match all time points when averaging the trials.

Figure 4-5 illustrates oil (ANS and IFO 120) lens growth and oil thickness decay as a function of time. Oils initially spread very quickly, but as the oil becomes thinner the rate of spreading slows as it approaches the walls of the basin. Heavy oils (IFO 120) are more viscous than medium grade oils (ANS); therefore heavy oil spreads more slowly on

seawater. Oil spreading is greatly retarded on seawater contaminated with a surface film. The transport of oil due to interfacial tension gradients can result in re-thickening of the oil thin films and provides a resisting force to oil film thinning, which is termed the Marangoni effect (Schamm, 2005).

Oil spreading can be expressed as a power law function according to Tanner's Law (4-2):

$$R_L \propto t^n \quad (4-2)$$

where  $R_L$  is the radius of the oil lens,  $t$  is time, and  $n$  is power (a constant) that can be calculated from the slope of the line when the  $\ln(R_L)_t$  is plotted as a function of  $\ln(t)$  (He & Hadjiconstantiou, 2003). This concept was illustrated in Figure 4-6 for both ANS and IFO 120. A summary of regression analysis performed on the  $n$ -power plots for oils (ANS & IFO 120) spreading on clean and contaminated (surface film) seawater is presented in Table 4-2. The  $n$ -value was determined from the slope ( $n$ ) of the line. The kinetics investigations of ANS and IFO 120 spreading on clean seawater produced similar  $n$ -values of 0.57 and 0.56 respectively. The kinetics investigations of spreading for ANS and IFO 120 on seawater in the presence of a horizontal interfacial gradient were slowed down and the  $n$ -values were reduced to 0.22 and 0.34 respectively. Therefore, the kinetics of oil spreading can be greatly controlled by an interfacial gradient acting in opposition to the oil expanding on the seawater surface. ANOVA produced statistically significant  $p$ -values  $< 0.05$  for the  $n$ -power plots, which rejects the null hypothesis that the examined variables are unrelated.

**Table 4-2:** Experimental conditions and regression analysis of oil spreading kinetics.

	#Trials	Temp.	Salinity	oil	<i>n</i> -power			1 <sup>st</sup> order Kinetics		
		°C	ppt	(g)	ln(R <sub>t</sub> ) against ln(t)			ln(h <sub>t</sub> ) against t		
Treatment		Ave±Stdev	Ave±Stdev	Ave±Stdev	<i>Intercept</i>	<i>n</i> mm·s <sup>-1</sup>	r <sup>2</sup>	<i>Intercept</i>	- <i>k</i> s <sup>-1</sup>	r <sup>2</sup>
ANS	3	18.0±0.3	31.2±0.1	12.9±0.1	5.242	0.574	0.991	5.77	-0.66	0.843
ANS-SF	2	20.6±0.3	31.2±0.1	12.8±0.0	3.870	0.222	0.981	6.90	-1.28E-02	0.843
IFO 120	2	19.0±0.0	31.3±0.1	14.2±0.1	4.522	0.556	0.978	6.36	-3.13E-01	0.863
IFO 120-SF	3	19.1±1.2	31.2±0.1	14.3±0.2	2.654	0.320	0.796	0.369	-9.00E-04	0.968

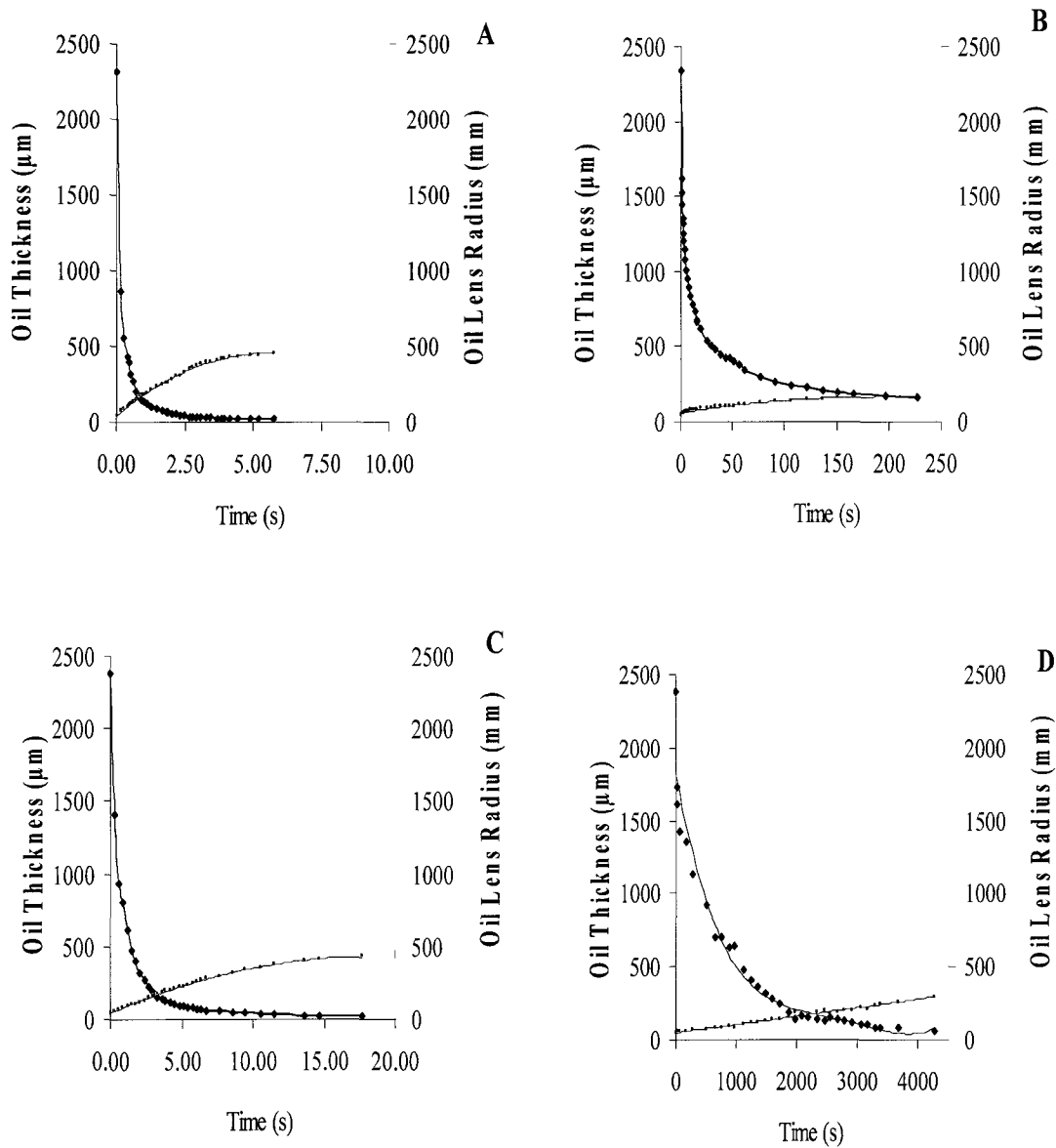


**Figure 4-5:** A plot of Lens growth and oil thickness decay as a function of time A) ANS spreading on clean seawater, B) ANS spreading on seawater with surface film, C) IFO 120 spreading on clean seawater, and D) IFO 120 spreading on seawater with surface film.

The kinetic model proposed  $\ln(h_t) = \ln(h_0) - kt$  (Chapter 2.62) was tested and the results are illustrated in Figures 4-7 and 4-8. Table 4-2 summarizes the intercepts, rate

coefficient, and coefficient of determination ( $r^2$ ) for the first order relationships. The ANOVA produced statistically significant  $p$ -values  $<0.05$  for the linear plots, which rejects the null hypothesis that the examined variables are unrelated. The rate coefficients ( $-k$ , the slopes of the curves) were  $-0.66$  and  $-3.13 \times 10^{-1} \text{ s}^{-1}$  for ANS and IFO 120 spreading on clean seawater respectively (Table 4-2). Surface film formation at the oil-seawater interface greatly reduces  $k(s)$  by  $\sim 50$  to  $300$  times for ANS and IFO 120 respectively compared to  $k(s)$  produced from the oils spreading on clean seawater. As evident from the data set, IFO 120, the most viscous oil spreads at a slower rate ( $\sim 2$  times slower) on clean seawater compared to ANS. The interfacial gradient concentration used in this study was  $\sim 0.008 \text{ mL/m}^2$  or  $0.08 \text{ L/hectare}$ . This coverage is approximately three orders of magnitude below a typical  $50 \text{ L/hectare}$  marine coverage recommended for dispersants (Nedwed & Coolbaugh, 2008). Given the fact that a very low concentration of horizontal interfacial gradient can greatly affect oil spreading rates on seawater, it is probable that more concentrated surface films (due to dispersant overspray) could affect oil dispersant effectiveness in wave tanks.

During the experiment, observations were noted such as when a surface film was present on seawater, oil could be herded toward any introduced dynamic flow such as a mobile fumehood arm situated next to the lab basin. Vibrational noise from the fumehood arm, even when turned off, lying next to the basin would create virtually non-visible active motion on the water surface. This motion appeared to move the films next to the oil, thus further slowing the spread of oil. As a result, the oil lens moved around the basin and appeared to mimic the vibrations. These conditions were corrected in order to evaluate horizontal gradient interference on oil spreading. Surface films can affect the

rate of oil spreading on seawater and could potentially affect chemical dispersant effectiveness in wave tank seawater.

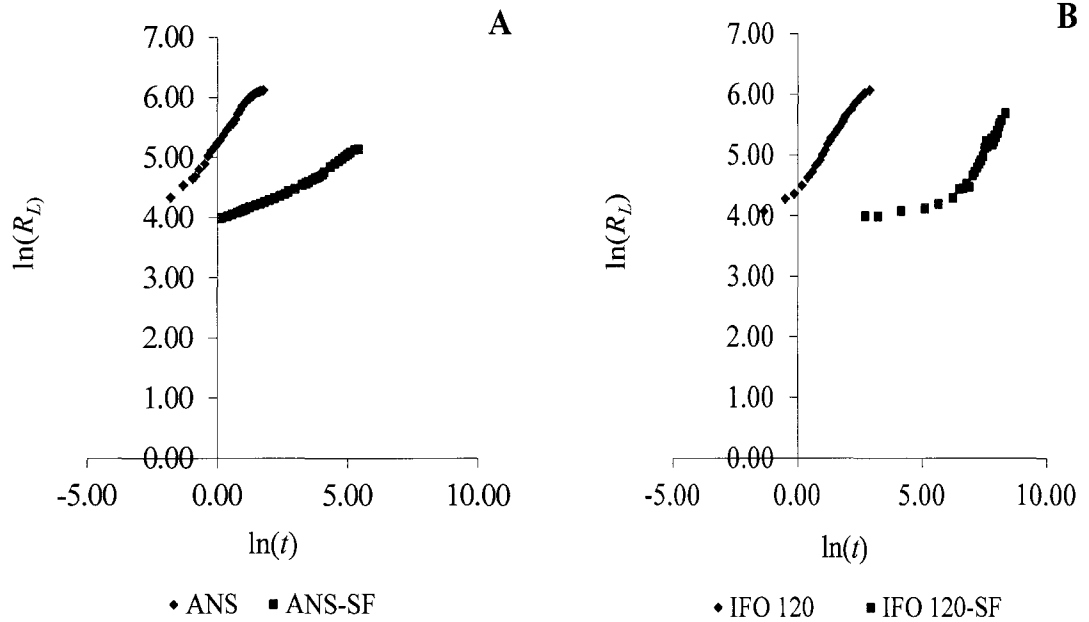


**Figure 4-6:** Logarithmic plots of the spreading kinetics of oil on clean seawater and seawater with surface film A) ANS and B) IFO 120.

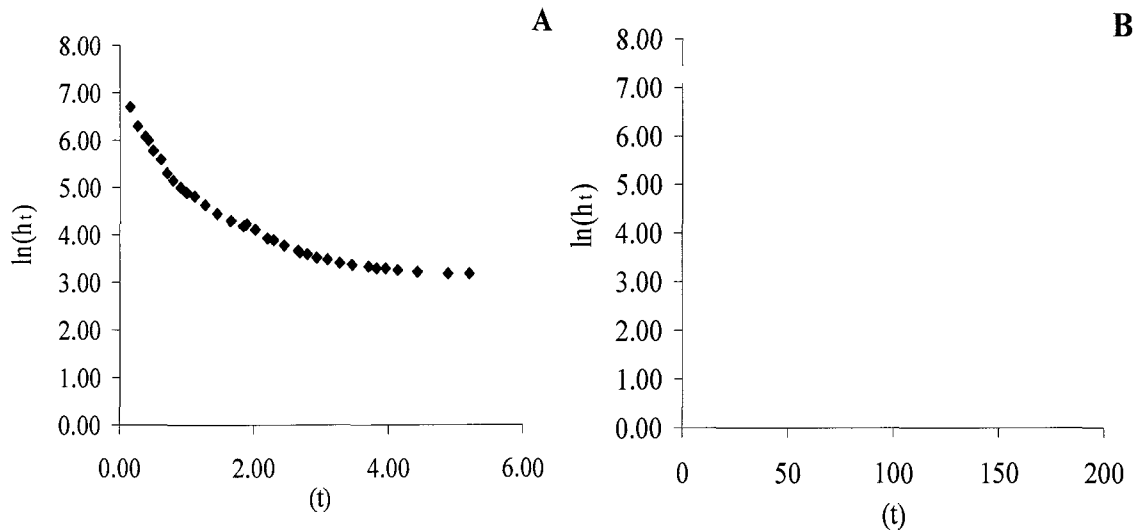


**Figure 4-7:** First order kinetics plots of ANS spreading on A) clean seawater & B) seawater with a surface film.

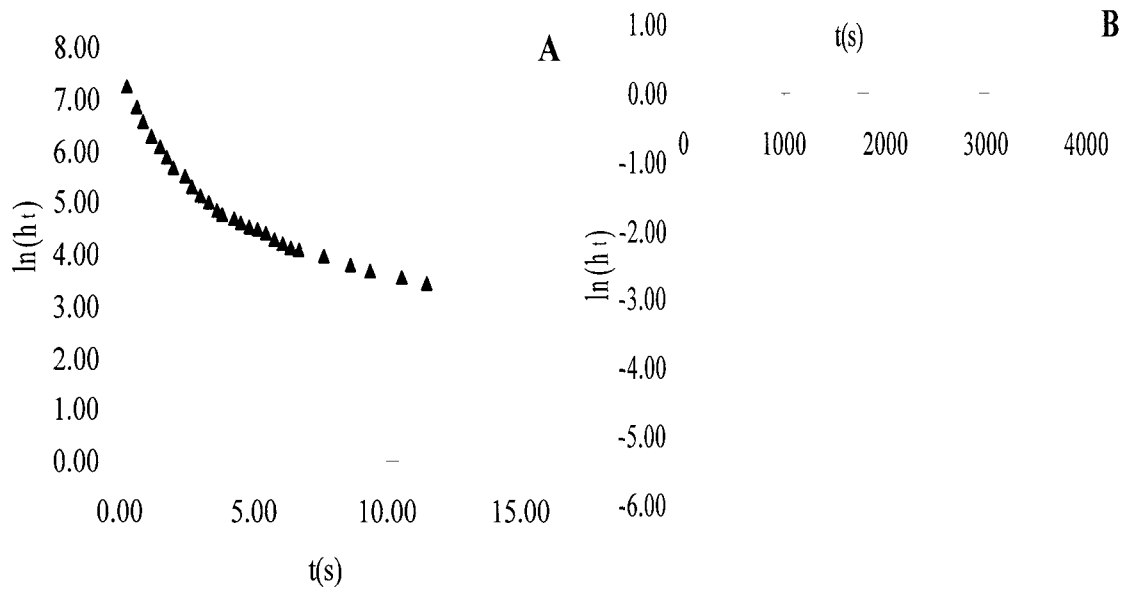


**Figure 1:** First order kinetics plots of IFO 120 spreading on A) clean seawater & B) seawater with a surface film.

#### ***4.5 The Effect of Oil Dispersant Overspray on Oil Dispersant Effectiveness***

ANS was selected for the oil dispersant overspray (surface film interference) studies, because it is easy to disperse with chemical dispersants and would provide adequate results for comparison purposes. The wave tank experimental conditions are presented in Table 4-3.

The raw statistically treated hydrocarbon and interfacial tension data for all treatments are displayed in Tables A10-A13 (Appendix A). The results are presented as the average values ( $n=3$  trials per treatment) from two locations (6 & 10 m) and three depths (5, 75, and 145 cm) in the wave tank. Figures 4-9 & 4-10 graphically display temporal and spatial profiles of interfacial tension and hydrocarbon levels for dispersed oil at 6 and 10 m from oil release respectively, for three treatments: A) natural

attenuation, no dispersant and no surface film; B) oil dispersed with Corexit 9500A, no surface film; and C) oil dispersed with Corexit 9500 (overspray, surface film effect).

Both low hydrocarbon levels and consistently high constant interfacial tension levels (Figures 4-9A) illustrated that ANS is poorly dispersed under natural conditions. In addition, visible observations demonstrated that naturally dispersed oil remained mostly on the surface as large visible droplets (Figure 4-11) and it was rapidly transported by waves downstream where it sticks to the walls and wave absorbers of the wave tank.

**Table 4-3:** Wave tank experimental conditions (NA-no application).

<b>Treatment#</b>	<b>Surface Film (g)</b>	<b>Dispersant (g)</b>	<b>Oil Mass(g)</b>	<b>AirTemp. (°C)</b>	<b>Salinity (ppt)</b>	<b>Seawater Temp. (°C)</b>
1	NA	11.93	231.72	20.0	29.5	16.6
2	NA	NA	254.09	19.9	29.6	18.7
3	50.04	11.92	265.79	19.5	29.8	17.1
4	NA	12.25	274.51	20.1	29.4	18.3
5	NA	NA	251.22	20.0	27.4	19.0
6	51.81	11.94	263.60	21.3	27.1	19.1
7	NA	11.93	265.00	25.5	27.3	18.7
8	NA	NA	255.90	16.5	29.1	15.0
9	51.98	12.01	266.46	20.8	29.3	15.7
Average	51.28	12.00	258.70	20.4	28.7	17.6
Stdev	1.07	0.13	12.44	2.3	1.1	1.5

The attenuation of ANS in the wave tank seawater can now be compared to the ANS lab basin studies. It was evident from the interfacial tension values consistently nearing background levels (Figure 4-9A & 4-10A) that surface films from oil application to seawater are not an issue in large scale wave tanks. The large body of seawater and larger surface area appears to minimize surface film formation from oil application. This indicates that large scale wave tanks more naturally model oil applied to seawater compared to surface film formation from oil application on lab basin seawater. Figure 4-10 (A&B) illustrates that for both natural and chemical dispersion of oil, both the hydrocarbon and interfacial tension values begin to approach equilibrium at all depths around 15 minutes. However; this amalgamation of both the chemical and physical values was delayed until ~60 minutes, when ANS was dispersed with surface film interference (simulated oil dispersant overspray). At the 60 minute time point, the effect of the surface film subsides leaving an increase in hydrocarbon levels (~20%) compared to chemically dispersed ANS. At 6 m from oil release the hydrocarbon results (Figure 4-9 B&C) appear similar for chemically dispersed oil in the wave tank seawater with and without surface film interference. However; the interfacial tension profiles at the same location are quite different showing a greater reduction in measurements from 5 to 75 cm depths. At 10 m, both the temporal and spatial profiles of hydrocarbon and interfacial tension levels are distinctly different for chemically dispersed ANS in wave tank seawater with surface film interference compared to without (Figures 4-10 B&C). In the first 30 minutes of experimental operations, 10 m downstream, hydrocarbon levels are ~3 times higher at the surface down to 75 cm of the water phase for chemically dispersed oil with simulated dispersant overspray (surface film) interference compared to without.

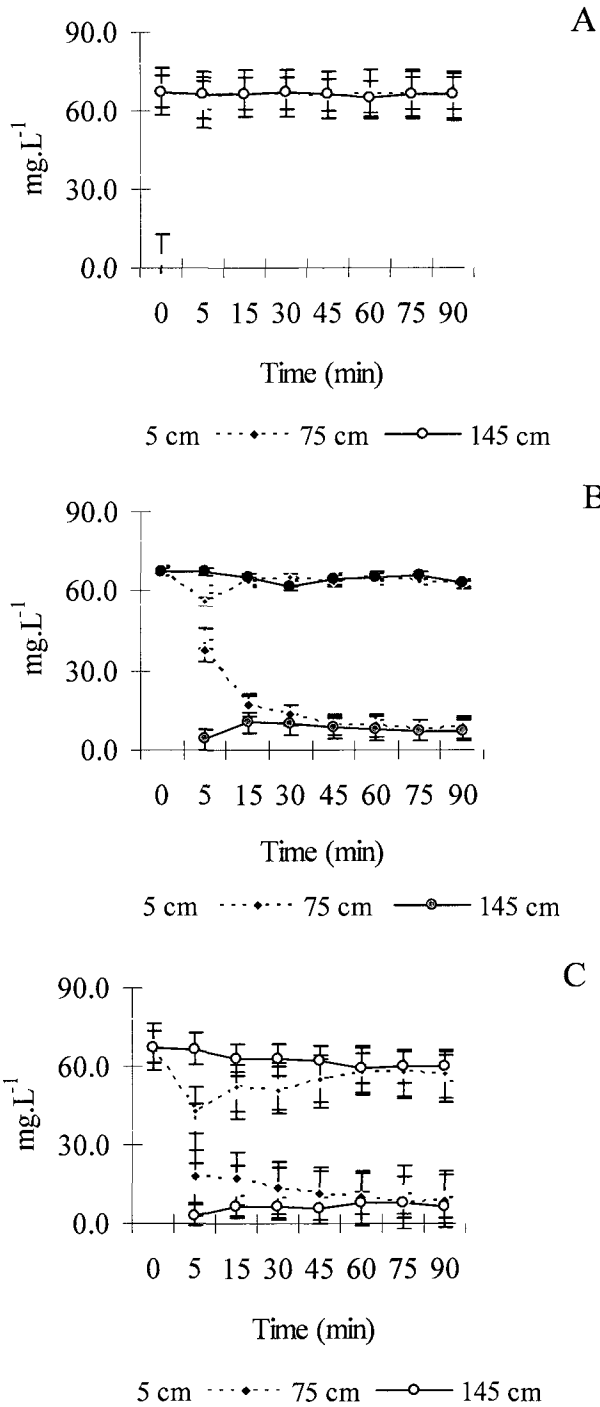


**Figure 4-9:** Temporal and spatial plots of average (n=3) hydrocarbon and interfacial tension levels 6m from oil release: A) ANS naturally attenuated; B) ANS dispersed with Corexit 9500; and C) surface film interference/ANS Dispersed with Corexit 9500.

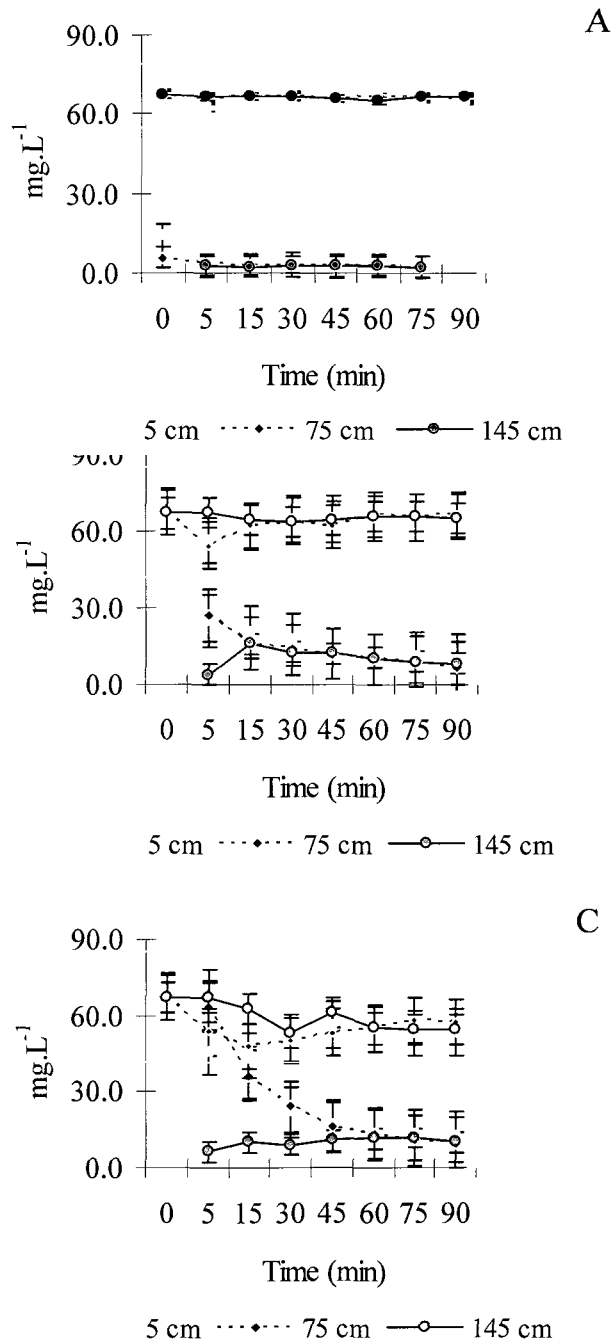


**Figure 4-10:** Temporal and spatial plots of average (n=3) hydrocarbon and interfacial tension levels 10m from oil release: A) ANS naturally attenuated; B) ANS dispersed with Corexit 9500; and C) surface film interference/ANS Dispersed with Corexit 9500.

According to Lunel (1995), oil droplets  $>70\mu\text{m}$  in size are considered to be suspended not dispersed, they are likely prone to buoyant forces, and they have potential to rise to the surface. International Maritime Organization Regulators set a limit of  $<15$  mg/L for oil bilge discharge from ships, a concentration at which oily sheens are believed not to occur (Fraser et al., 2006). These two references suggest that oily sheens are most likely to occur when hydrocarbon levels are  $>15$  mg/L and oil droplets are  $>70$   $\mu\text{m}$  in size. Oily sheen formation appeared evident from a photo (Figure 4-11A) taken during the experiment when ANS was dispersed in the presence of oil dispersant overspray (surface film contamination) and by the elevated levels ( $>20$  mg/L up to 30 minutes in operations) of hydrocarbon (5 to 75 cm) in samples taken 10 m downstream from oil release (Figure 4-10 C).

In the initial 30 minutes of operation, the simulated dispersant overspray (surface film) interferes with and appears to underestimate the oil dispersant effectiveness. In this situation, using effluent from the wave tank to evaluate fate (biodegradation) and effects (fish toxicity) of dispersed oil could lead to confounding results. In addition, dispersant overspray (surface film) in closed systems, like wave tanks could affect decisions on new oil dispersant formulations. The issue with oil dispersant overspray is restricted to test facilities, because of boundaries (walls) that provide an ideal environment for surface film formation. This situation does not mimic the natural environment, since there are no boundaries present in the open sea. Dispersant overspray in the natural environment would probably dilute due to continuous spreading in all directions thus minimizing its effects on oil dispersant effectiveness.

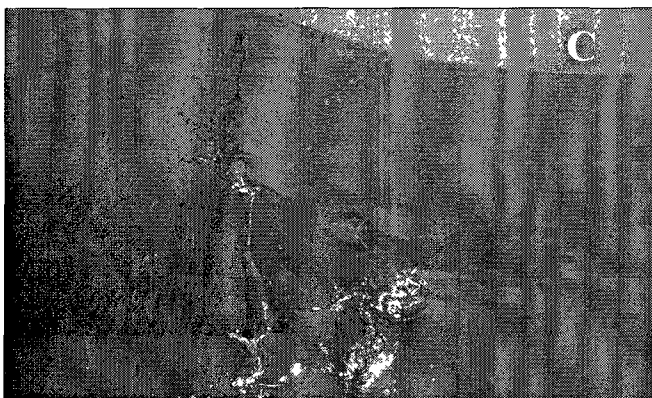
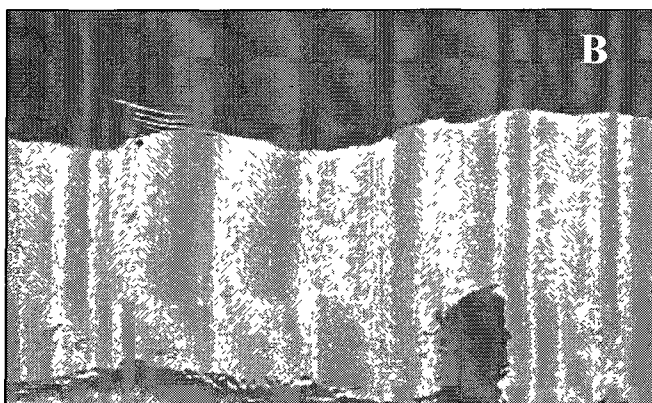
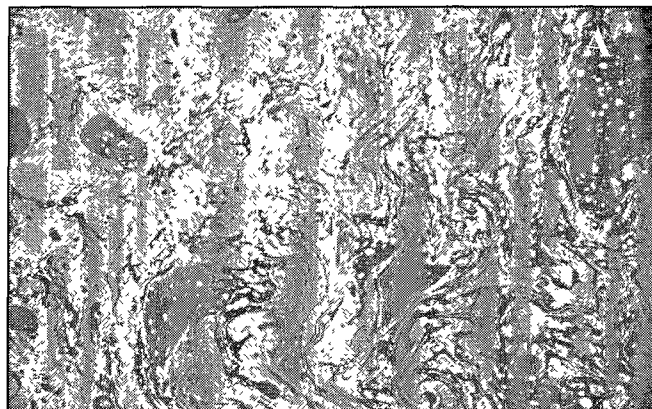


**Figure 4-11:** Photos of visual observations: A) intense oily sheen formation of chemically dispersed oil with surface film interference, B) chemical dispersion of oil, and C) natural attenuation of oil.

Figure 4-12 shows GC-FID chromatograms of a known concentration of Corexit 9500 extracted from seawater and an ANS standard, which are compared to sample

extract chromatograms at 15 minutes of operations for all three wave tank treatments. It is clearly evident from the GC-FID chromatograms that the surface film generated from Corexit 9500 doesn't contribute or bias the hydrocarbon levels detected in the dispersed oil samples.

The rate of oil entrainment can be viewed as the dispersion of oil in the wave tank seawater, which follows first-order kinetics. Thus, the oil mass at any time is expressed as ( $m_t$ ) but is equal to the difference between the mass at that time ( $m$ ) and the terminal mass value achieved at the end of oil dispersion in the wave tank ( $m_{\infty}$ ). With the rate of oil entrainment expressed as  $dm_t/dt$ . Thus:

$$\frac{dm_t}{dt} = -k(m_t) \quad (4-3)$$

The  $k$  is the first order entrainment rate constant and has reciprocal time units. An integrated rate law expression can be derived by integrating the above expression between the limits of thickness of initial thickness,  $h_{t_0}$  to the thickness at any time,  $h_t$  and; between the limits of initial time,  $t_0$  and any time,  $t$ :

$$\int_{m_t}^{m_{t_0}} \frac{dm_t}{m_t} dh_t = - \int_{t_0}^t k(d_t) \quad (4-4)$$

The integration is solved as:

$$\ln(m_t) = \ln(m_0) - k(t - t_0) \quad (4-5)$$

The initial time is taken to be equal to zero so that  $(t - t_0) = t$ . The solution can be rearranged to give:

$$\ln(m_t) = \ln(m_0) - kt \quad (4-6)$$

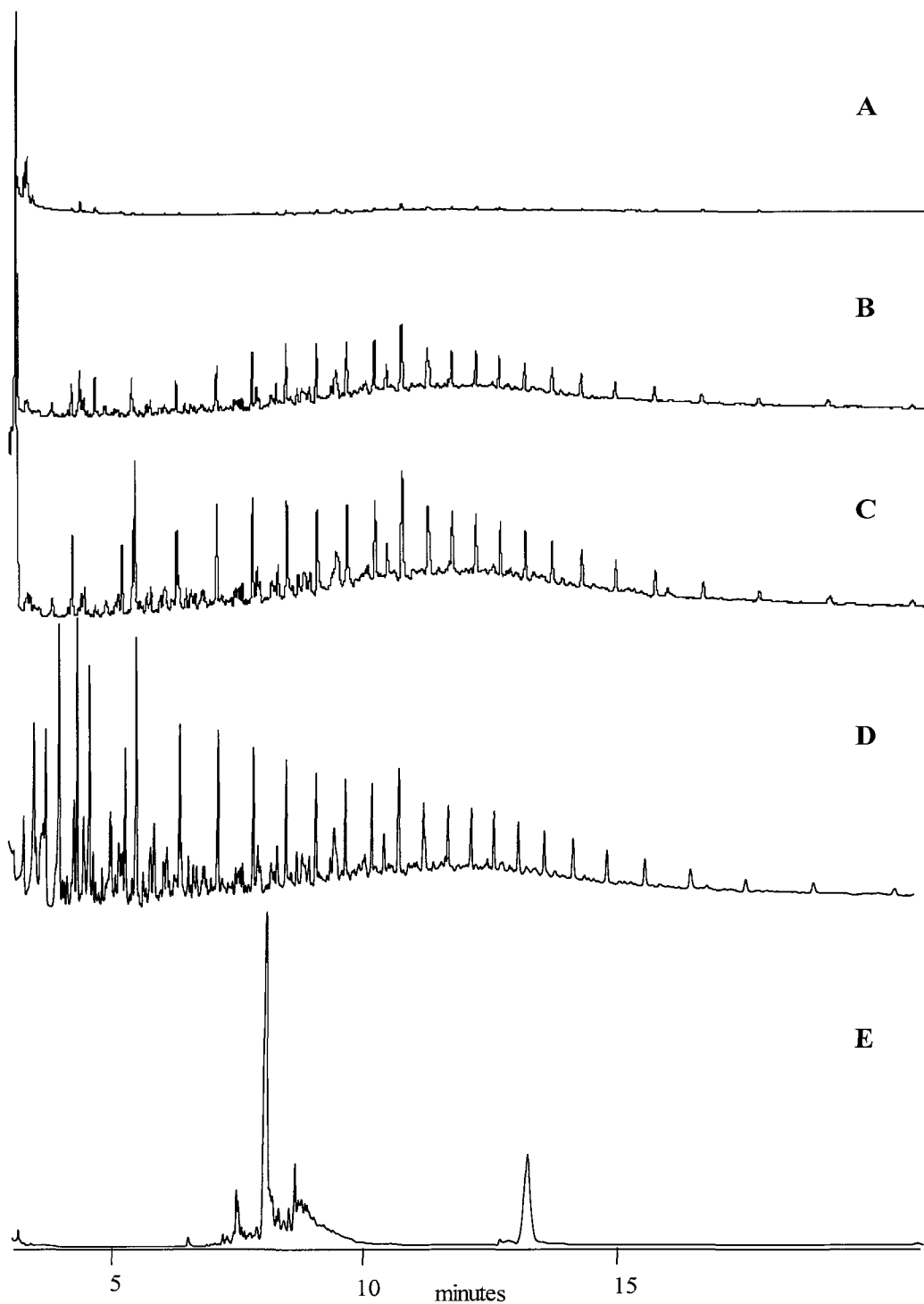


**Figure 4-12:** GC-FID chromatograms A) naturally dispersed oil, B) chemically dispersed oil, C) chemically dispersed oil in presence of surface films, D) ANS standard and E) 25 ppm Corexit 9500 in seawater.

Upon rearrangement the solution expresses the integrated rate law as an equation of a line,  $y = mx + b$ , so that a plot of the natural logarithm of oil mass against time should yield a straight line with the first-order reaction rate constant as the negative value of the slope. The line thus predicts the value of the mass of oil at any time *not* in the time period approaching the terminal mass of oil. Comparing  $k$  values for oil entrainment in clean and contaminated (surface film) seawater aids to quantitatively determine the effects that a surface film has on oil entrainment. The reaction rate constant is constant so long as there is no catalytic effect and/or temperature change. The value of  $k$  depends on temperature, therefore the oil entrainment experiments were carried out during a seasonal period where seawater has minimal temperature changes.

To simplify calculations the average mass of the oil (258.7 g, Table 4-3) was taken as  $m_o$ . Hydrocarbon results varied most dramatically 10 m from oil release, therefore results from this sampling location were averaged for all depths for the two treatments of chemically dispersed oil and chemically dispersed oil with surface film interference (simulated dispersant overspray). Concentrations for each of the time points were converted to masses based on a per litre of sample, which represent  $m_t$ . The data generated from the calculations are presented in Table 4-4 (Example Calculation 4, Appendix B). Figure 4-13 illustrates the 1<sup>st</sup> order kinetic of chemically dispersed oil and chemically dispersed oil with oil dispersant overspray (surface film interference). Regression analysis produced  $r^2$  values of 0.983 and 0.860 and  $-k$  values of  $-9.80 \times 10^{-3}$  and  $-1.57 \times 10^{-2} \text{ min}^{-1}$  for chemically dispersed oil and chemically dispersed oil with surface film interference respectively. There is a deviation (46% difference, Example Calculation 5 Appendix B) in the rate constant of chemically dispersed oil with surface

film interference compared to chemically dispersed oil, but the process still follows 1<sup>st</sup> order kinetics.

**Table 4-4:** First order kinetics data for dispersed oil in wave tank seawater with and without surface film interference.

		ANS/Corexit 9500			ANS /Corexit 9500 (Surface Film)		
		Ave (all depths) 10 m Downstream From Oil release			Ave (all depths) 10 m Downstream From Oil Release		
Time		Oil	$\ln(m_t)$		Oil	$\ln(m_t)$	
(min)	mg/L	grams		mg/L	grams		
0		258.70			258.70		
5	18.6	0.0186	-3.99	45.9	0.0459	-3.08	
15	17.5	0.0175	-4.05	28.1	0.0281	-3.57	
30	14.5	0.0145	-4.23	18.4	0.0184	-3.99	
45	12.1	0.0121	-4.41	14.6	0.0146	-4.23	
60	10.1	0.0101	-4.60	12.8	0.0128	-4.36	
75	9.6	0.0096	-4.64	12.0	0.0120	-4.43	
90	8.3	0.0083	-4.79	10.7	0.0107	-4.54	

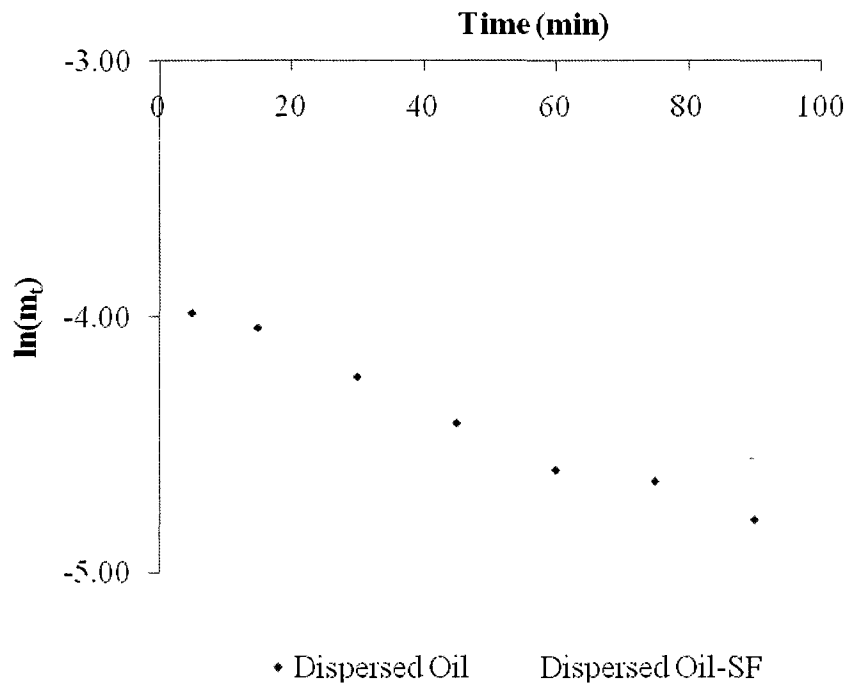


**Figure 4-13:** 1<sup>st</sup> Order kinetics plot of dispersed oil in wave tank seawater with/without surface film interference.

The dispersed oil in the seawater phase of a dynamic wave tank (closed system) can be expressed as diffusion controlled long-time limit adsorption (4-7):

$$\gamma(t) - \gamma_e = \frac{\Gamma^2 RT}{[C_o \sqrt{\pi D t}]} \quad (4-7)$$

where  $\gamma(t)$  and  $\gamma_e$  are the interfacial tension at time ( $t$ ) and interfacial tension at equilibrium ( $t \rightarrow \infty$ ) respectively,  $\Gamma^2$  equilibrium surface adsorption,  $R$  is the ideal gas constant,  $T$  is the temperature in degrees Kelvin,  $C_o$  is the initial surfactant concentration, and  $D$  is the diffusion coefficient. This approach has been used by others to examine natural surface film adsorption kinetic at sea (Pogorzelski & Kogut, 2001; Mercedes et al., 1999; Liu et al., 2005). Average interfacial tension values over time for chemically

dispersed oil without and with surface film interference were used. For diffusion controlled long-time limit adsorption, a linear relationship exists between  $\gamma(t)$  and  $\frac{1}{\sqrt{t}}$  if the disperse oil process is driven by diffusion and if it is non-linear then a mixed diffusion gradient barrier mechanism is at work (Liu & Messow, 2000; Liu et al., 2005). A linear plot of these variables is illustrated in Figure 4-14 A & B for chemically dispersed oil at the surface (surface- 5cm, sample drawn in presence of waves) and in the subsurface (average interfacial tension values for all sampling depths). However, in the case of dispersed oil in the presence of a horizontal interfacial gradient (surface film), the process is driven by a mixed diffusion horizontal gradient barrier mechanism and deviates from linearity, which is more apparent in the subsurface of the water phase. This revealed that the horizontal interfacial gradient interferes with the dispersed oil in the dynamic wave tank seawater. In the initial stages (first 30 minutes) of operations the horizontal interfacial gradient effectively prevented the oil from breaking into smaller droplets in the dynamic wave tank seawater, thus underestimating the oil dispersant effectiveness.

Regression analysis (n=7) of the subsurface plots (Figure 4-14 B) produced  $r^2$  values of 0.949 and 0.010 for chemically dispersed oil and chemically dispersed oil with a horizontal interfacial gradient respectively. ANOVA produced  $p$ -values of  $2.08 \times 10^{-4}$  and  $8.28 \times 10^{-1}$  and standard errors of 0.38 and 1.56 for chemically dispersed ANS and ANS dispersed with surface film interference respectively. For  $p$ -values  $> 0.05$ , one accepts the null hypothesis that the examined variables are unrelated. This was evident in the case where chemically dispersed ANS was affected by the presence of a simulated dispersant overspray to generate a surface film. Chemically dispersed oil with overspray

(surface film interference) can affect interfacial tension and hydrocarbon dispersed oil profiles, which are more pronounced at 10m downstream from oil release.

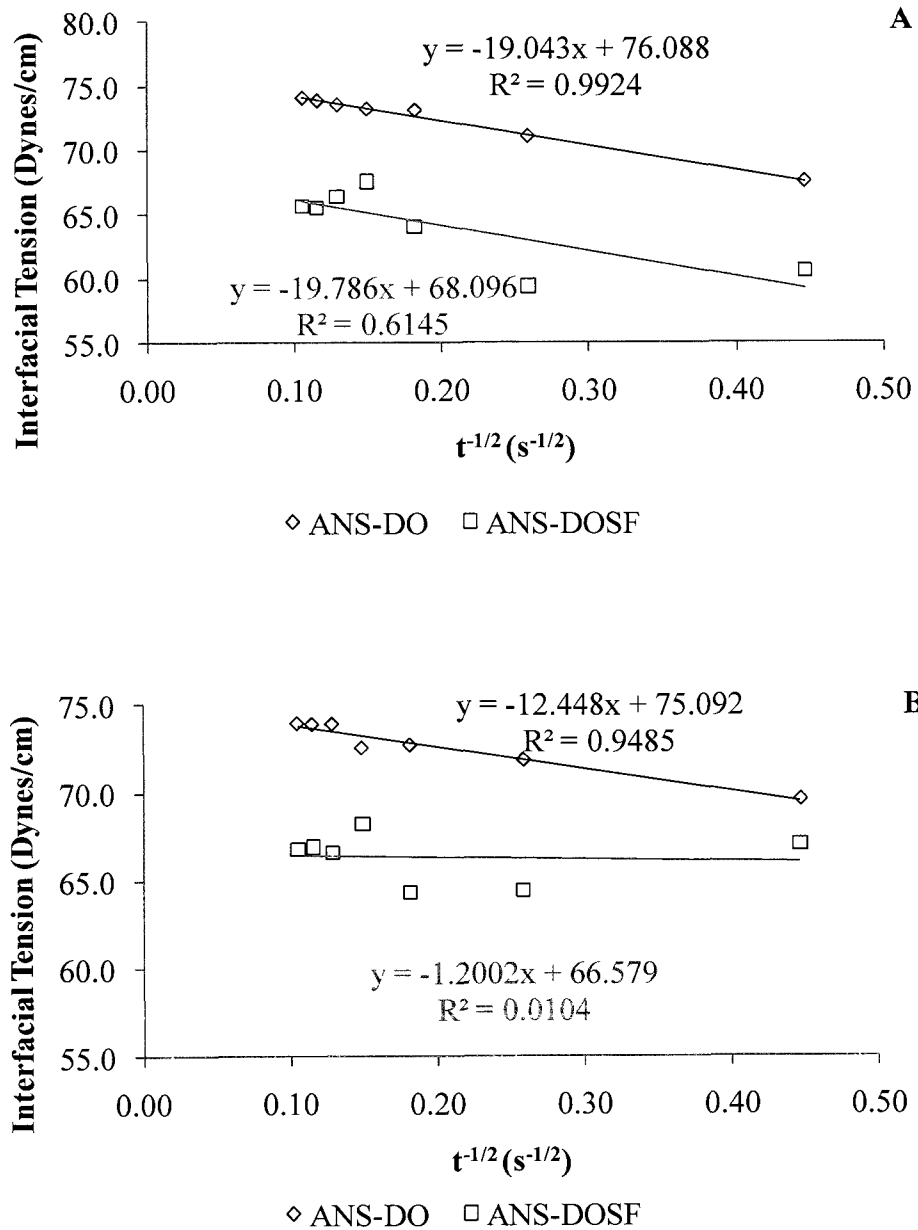


**Figure 4-14:** A plot of interfacial tension as a function of the square root of time ( $s^{1/2}$ ) for dispersed oil & dispersed oil with horizontal interfacial gradient interference (A) surface and (B) subsurface.

Overall, the presence of oil dispersant overspray underestimates oil dispersant effectiveness in a closed system dynamic wave tank facility. These effects were most apparent in the first 30 minutes of operations. In a closed system, the dispersed oil remains in the system and the continuous mixing energy eventually overcomes the horizontal interfacial gradient. In an open system (flow-through dynamic wave tank), the dispersed oil is transported out of the system illustrating subsurface spatial distribution. The effects from a horizontal interfacial gradient would probably be minimized over the same time range in an open system wave tank. Open system wave tanks (simulate sea current) dilute the dispersed oil in the wave tank seawater. Interfacial tension measurements are ideal to assess surface film formation in a static environment and can adequately profile the effects of oil dispersant overspray (surface film interference) on oil dispersants effectiveness in the dynamic wave tank seawater.

## **Chapter 5**

### **Summary and Conclusions**

#### ***5.1 Surface Film Formation***

The adsorption process of selected crude oils, ALC and ANS, on static seawater in a lab basin was demonstrated to follow diffusion-controlled short time limit adsorption kinetics. This occurrence was not apparent for IFO 120 on seawater during the four hour study. The experimental diffusion coefficients for ALC and ANS were on the order of  $10^{-6}$  and  $10^{-7}$   $\text{cm}\cdot\text{s}^{-1}$  which are two three orders of magnitude different compared to literature values. The difference in  $D$ -values is considered to be due to differences in factors such temperature of seawater, weathering of the oils and chemical and physical

composition of the oils. Under static conditions, the adsorption of surface films from oil applied to seawater was driven by diffusion. When dispersant was added to the oil there was an immediate drop in interfacial tension resulting in surface film formation. Interfacial tension provides adequate evaluation of horizontal interfacial gradient formation at the oil-seawater interface.

### ***5.2 Oil Spreading Rates***

Horizontal interfacial gradients formed using Corexit 9500 in a lab basin at the oil-seawater interface can affect oil spreading rate. The kinetics investigations of ANS and IFO 120 spreading on clean seawater evaluated with the *n*-Power Law produced similar *n*-values of 0.57 and 0.56 respectively. Horizontal interfacial gradients at the oil-seawater interface slowed the spreading of ANS and IFO 120, thus reducing the *n*-values to 0.22 and 0.34 respectively. Therefore, the kinetics of oil spreading can be greatly controlled by interfacial molecular arrangement at the oil-seawater interface.

Crude oil horizontal spreading follows 1<sup>st</sup> order kinetics on clean and contaminated (surface film) seawater in a static basin environment. The rate coefficients (*-k*) were -0.66 and  $-3.13 \times 10^{-1} \text{ s}^{-1}$  for ANS and IFO 120 spreading on clean seawater. IFO 120 the denser, more viscous of the two oils has a slower spreading rate on seawater compared to ANS. Surface film formation at the oil-seawater interface greatly reduced *k*(s) by ~ 50 to 300 times for ANS and IFO 120 respectively compared to *k*-values for these oils spreading on clean seawater. Horizontal interfacial gradients can greatly affect the rate of oil spreading, thus have the potential to affect oil dispersant effectiveness in dynamic wave tank seawater.

### ***5.3 Oil Dispersant Effectiveness***

It was apparent from the interfacial tension approaching background seawater levels that oil application did not produce a surface film effect in the large scale wave tank. The wave tank naturally represented oil application to seawater compared to oil application that produced a surface film on seawater in the small-scale basin.

Visible observations revealed intense oily sheen formation when ANS was dispersed in wave tank seawater in the presence of a horizontal interfacial gradient. This was complimented by distinctly different hydrocarbon and interfacial tension profiles for both the chemical dispersion of ANS with and without horizontal interfacial gradient. In the first 30 minutes of experimental operations, 10 m downstream, hydrocarbon concentrations are 2 to 3 times higher at the surface (5 cm) down to 75 cm of the water phase for chemically dispersed oil with surface film intrusion compared to without. After 60 minutes of wave tank operations, the horizontal interfacial gradient subsides and contributes to oil dispersant-effectiveness.

ANS dispersed in clean and contaminated (simulated overspray, a surface film) seawater in the dynamic wave tank (closed system) follows 1<sup>st</sup> order kinetics. The rate coefficients were  $-9.80 \times 10^{-3}$  and  $-1.57 \times 10^{-2} \text{ min}^{-1}$  for chemically dispersed ANS and chemically dispersed ANS with surface film (simulated dispersant overspray) interference. However, there was a deviation (46% difference) in the regression slopes when ANS was dispersed in seawater in the presence of a horizontal interfacial gradient compared to clean seawater.

Chemically dispersed oil was driven by diffusion in dynamic wave tank seawater, which was expressed as long-time limit adsorption, producing a linear relationship

( $r^2=0.949$ ) between  $\gamma(t)$  and  $\frac{1}{\sqrt{t}}$ . However, in the case of dispersed oil in wave tank seawater in the presence of a horizontal gradient, the process was driven by a mixed diffusion-horizontal gradient mechanism and deviates from linearity ( $r^2=0.010$ ). This explains why the oil levels are higher near the surface (5 cm) to 75 cm depth, because of the repulsive effects of the horizontal interfacial gradient preventing the oil from breaking into smaller droplets and effectively dispersing into the seawater phase.

The presence of an undetected horizontal interfacial gradient prior to oil dispersant effectiveness tests in the wave tank facility can greatly affect the decision making process on new dispersant formulated for use in the marine environment. The presence of interfacial gradient, as the result of dispersant overspray, can produce an unnatural model of the fate and effects of dispersed oil. The unnatural effects of dispersed oil could over estimate the risks of oil dispersant (i.e. higher hydrocarbon levels in the seawater phase) used in the marine environment. Interfacial tension measurements provide evidence of surface film formation and its affects on oil spreading on static lab basin seawater and an adequate profile of surface film interference (overspray) on oil dispersants effectiveness in a dynamic large scale wave tank.

## **Bibliography**

Abdurahman, H.N., & Yunus, R.M. *International Journal of Chemical Technology*.

**2009**, 1 19-25.

Allered, B.J., & Brown, G.O. *Environmental Geosciences*. **2001**, 8, 92-109.

ASTM D971 - 99a Standard Test Method for Interfacial Tension of Oil Against Water by the Ring Method. 2002, 1-7.

Atlas, R.M., & Bartha, R. *Canadian Journal of Microbiology*. **1972**, 18, 1851-1855.

Blondina, G. J., Singer, M. M., Lee, I., Ouano, M. T., Hodgins, M., & Tjeerdema, R. S. *Spill Science and Technology Bulletin*. **1999**, 5(2), 127-134.

Chandrasekar, S., Sorial, G.A., & Weaver, J.W. *Journal of Marine Science*. **2006**, 63, 1418-1430.

Cole, M., King, T., & Lee, K. *Canadian Technical Report of Fisheries and Aquatic Sciences*. **2007**, 2733, 1-12.

Drelich, J., & Miller, J. *Annales Sectio*. **2000**, AA 7, 105-115.

Dutta, T.K., & Harayama, S. *Environmental Science and Technology*. **2001**, 35, 102-107.

Fay J.A. The Spread of Oil Slicks on a Calm Sea In: Oil on the Sea; D. P. Hoult, Ed.; New York: New York, 1969; pp 53-63.

Flaming, J., Knox, R., Sabatini, D., & Kibbey, T. *Vandose Zone Journal*. **2003**, 2, 168-176.

Fraser, G.S., Russel, J., & Won Zharen, W.M. *Marine Ornithology*. **2006**, 24 147-156.

Hale, M., & Mitchell, J. *Marine Ecology Progress Series*. **1997**, 147, 269-276.

He, G., & Hadjiconstantiou, N.G. *Journal of Fluid Mechanics*. **2003**, 497, 123-132.

- IP, S.W., & Toguri, J.M. *Journal of Material Science*. **1994**, 29, 688-692.
- Kanicky, J.R., Lopez-Montilla, J., Pandey, S., & Shah, D. *Surface Chemistry in the Petroleum Industry*. In *Handbook of Applied Surface and Colloidal Chemistry*; K. Holmberg, Ed.; New York: New York, 2001; pp.251-267.
- King, T., Lee, K., Clyburne, J., & Li, Z. *Abstract of Spatial and Temporal Distribution of Dispersed Oil in a Wave Tank Facility*, Proceeding of 33<sup>rd</sup> Arctic and Marine Oil Spill (AMOP) Technical Seminar on Environmental Contamination and Response, Halifax, Nova Scotia, June 8-10, 2010.
- Lessard, R.R., & Demarco, G. *Spill Science and Technology*. **2000**, 6(1), 59-68.
- Li Z, Lee K, Kepkay P, King T, Yeung W, Boufadel MC, Venosa A.D. Wave tank studies on chemical dispersant effectiveness: dispersed oil droplet size distribution. In *Oil Spill Response: A Global Perspective*; Davidson WF, Lee K, Cogswell A, Eds.; NATO Science for Peace and Security Series C: Environmental Security, Springer, 2008a; pp 143 – 157.
- Li, Z., Lee, K., King, T., Boufadel, M. C., & Venosa, A. D. *Marine Pollution Bulletin*. **2008b**, 56(5), 903-912.
- Li, Z., Lee, K., King, T., Boufadel, M. C., & Venosa, A. D. *Marine Pollution Bulletin*. **2009**, 58(5), 735-744.
- Li, Z., Lee, K., King, T., Boufadel, M., & Venosa, A. *Environmental Engineering Science*. **2009**, 26(9), 1407-1418.
- Liu, J., & Messow, U. *Colloidal Polymer Science*. **2000**, 278, 1-24.
- Liu, J., Zhang, C.H., Yang, C., & Messow, U. *Colloidal Journal*. **2005**, 67(3), 377-380.
- Liu, X., & Duncan, J.H. (2003). *Nature*. **2003**, 421, 520-523.

- Lunel, T. *Understanding the Mechanism of Dispersion Through Oil Droplet Size Measurement at Sea. In The Use of Chemicals in Oil Spill Response ASTM STP 1252*; Peter Lane, Ed.; Philadelphia: American Society for Testing and Materials, 2005, pp10-21.
- Lunel, T., & Lewis, A. *Optimization of Oil Spill Dispersant Use*, Proceeding of the International Oil Spill Conference, 1999; pp187-193.
- Maki, H., & Sasaki, T. *Journal Japan Society on Water Environment*. **1997**, 20(9), 639-642.
- Mercedes, G.M., Monroy, F., Ortega, F., Rubio, R. & Langevin, D. *Langmuir*. **1999**, 16(3), 1083-1093.
- NALCO. (2010). Corexit ingredients. 2010. <http://www.nalco.com/news-and-events/4297.htm> (accessed January 2011).
- Nedwed, T., & Coolbaugh, T. Do Basins and Beakers Negatively Bias Dispersant-Effectiveness Tests? Proceeding of the International Oil Spill Conference, 2008; pp 835-842.
- Pogorzelski, S., & Kogut, A.D. *Oceanologia*. **2001**, 43(4), 389-404.
- Quintero, C.G., Noïk, C., Dalmazzone, C., & Grossicord, J.L. *Oil and Gas Science Technology*. **2009**, 64(5), 607-616.
- Saylor, J.R. *Experiments in Fluids*. **2003**, 34, 540-547.
- Schamm, L. *Emulsions, Foam, and Suspensions: Fundamentals and Applications*; WILEY-VCH Verlag GmbH & Co. KGaA: Weinheim, Germany, 2005; pp 1-283.
- Singer, M., George, S., & Tjeerdema, R. *Archives of Environmental Contamination Toxicology*. **1995**, 29, 33-38.

- Singer, M., George, S., Jacobson, S., Lee, I., Weetman, L., Tjeerdema, R., & Sowby, M. *Ecotoxicology and Environmental Safety*. **1996**, 35, 183-189.
- Sterling Jr., M.C., Bonner, J.S., Page, C.A., Fuller, C.B., Ernest, A.N.S., & Autenrieth, R.L. *Environmental Science and Technology*. **2003**, 37(19), 4429-4434.
- Sterling Jr., M. C., Bonner, J. S., Ernest, A. N. S., Page, C. A., & Autenrieth, R. L. *Marine Pollution Bulletin*. **2004**, 48(9-10), 969-977.
- Stolle, C., Nagel, K., Labrenz, M., & Jürsen, K. *Biogeosciences Discussions*. **2010**, 7, 3153-3187.
- Vargaftik, B.N., Volkov, B.N., & Voljak, L.D. *Journal of Physical Chemistry Reference Data*. **1983**, 12(3), 817-820.
- Venosa, A., King, D., & Sorial, G. (2002). *Marine Pollution Bulletin*. **2002**, 7, 299-308.
- Yakata, N., Sudo, Y., & Tadokoro, H. *Chemosphere*. 2006, 64, 1885-1891.
- Ye, Z., Zhang, F., Han, L., Luo, P., Yang, J., & Chen, H. *Colloids and Surfaces A: Physicochemical and Engineering Aspects*. **2008**, 322 138-141.

**Appendix A**  
**Supporting Data**

**Table A1:** Interfacial tension and viscosity data (control for Surface Film Formation Studies).

	$\gamma$ (dynes/cm)				$\nu$ (cP)			
	*Trial #				*Trial #			
<b>Time (min)</b>	1	2	Ave	Stdev	1	2	Ave	Stdev
<b>0</b>	72.9	73.0	73.0	0.1	1.30	1.29	1.30	0.01
<b>10</b>	73.0	72.9	72.9	0.1	1.29	1.30	1.30	0.01
<b>30</b>	72.9	72.9	72.9	0.0	1.30	1.29	1.30	0.01
<b>60</b>	72.9	72.9	72.9	0.0	1.31	1.29	1.30	0.01
<b>120</b>	73.0	72.8	72.9	0.2	1.30	1.29	1.30	0.01
<b>180</b>	72.9	72.6	72.7	0.2	1.30	1.30	1.30	0.00
<b>240</b>	73.0	72.5	72.7	0.4	1.29	1.31	1.30	0.01

\*Trial 1 oil only, Trial 2 oil/dispersant

**Table A2:** Surface pressure and viscosity data for ALS (surface film formation).

	$\gamma$ (dynes/cm)						$\nu$ (cP)					
Time	Seawater Temperature (19.9±0.1 °C) Salinity (31.2±0.0 ppt)											
min	Trial#						Trial#					
	1	2	3	4	Ave	Stdev	1	2	3	4	Ave	Stdev
<b>0</b>	72.9	72.5	72.5	72.6	72.6	0.2	1.30	1.2	1.25	1.30	1.27	0.03
<b>10</b>	73.0	71.2	72.8	72.3	72.3	0.8	1.28	1.7	1.26	1.40	1.40	0.18
<b>30</b>	69.1	72.0	72.8	71.3	71.3	1.6	1.36	1.2	1.35	1.40	1.34	0.07
<b>60</b>	67.1	68.5	71.8	69.1	69.1	2.0	1.30	1.2	1.34	1.65	1.38	0.18
<b>120</b>	60.0	60.9	71.0	64.0	64.0	5.0	2.16	1.3	1.31	1.97	1.68	0.45
<b>180</b>	60.9	62.2	62.7	61.9	61.9	0.7	1.42	1.3	1.32	1.53	1.40	0.10
<b>240</b>	63.2	62.1	62.1	62.4	62.4	0.5	1.30	1.3	2.05	2.19	1.70	0.49

**Table A3:** Interfacial tension and viscosity data for ALS/dispersant (surface film formation)

	$\gamma$ (dynes/cm)					$\nu$ (cP)				
	Trial#					Trial#				
<b>Time</b>										
<b>(min)</b>	1	2	3	Ave	Stdev	1	2	3	Ave	Stdev
<b>0</b>	72.5	72.2	72.5	72.4	0.2	1.50	1.50	1.50	1.50	0.00
<b>10</b>	51.5	43.0	43.3	45.9	4.8	1.54	1.50	1.65	1.56	0.08
<b>30</b>	53.0	42.0	43.8	46.2	5.9	1.86	1.70	1.75	1.77	0.08
<b>60</b>	51.2	46.1	44.1	47.1	3.7	1.85	1.70	2.15	1.90	0.23
<b>120</b>	51.5	44.4	42.8	46.2	4.6	1.50	2.25	1.87	1.87	0.38
<b>180</b>	51.0	43.1	40.1	44.8	5.6	1.60	1.80	2.91	2.10	0.71
<b>240</b>	47.9	43.2	41.5	44.2	3.3	1.55	1.80	2.87	2.07	0.70

**Table A4:** Average interfacial tension and viscosity data (ANS surface film formation).

	$\gamma$ (dynes/cm)					$\nu$ (cP)				
	Seawater Temperature (20.87±0.06 °C) Salinity (31.1±0.1 ppt)									
	Trial#					Trial#				
Time (min)	1	2	3	Ave	Stdev	1	2	3	Ave	Stdev
<b>0</b>	72.5	72.6	72.7	72.6	0.1	1.51	1.47	1.51	1.50	0.02
<b>10</b>	72.5	69.7	66.1	69.4	3.2	1.50	1.50	1.53	1.51	0.02
<b>30</b>	72.5	67.9	67.7	69.4	2.7	1.50	1.51	1.58	1.53	0.04
<b>60</b>	70.1	68.8	66.3	68.4	2.0	1.51	1.48	1.53	1.51	0.03
<b>120</b>	68.7	67.8	66.0	67.5	1.4	1.54	1.47	1.54	1.52	0.04
<b>180</b>	65.2	67.9	66.9	66.7	1.4	1.52	1.51	1.52	1.52	0.01
<b>240</b>	64.5	65.9	60.7	63.7	2.7	1.51	1.48	1.51	1.50	0.02

**Table A5:** Kinetics data (Ave±Stdev) for ANS spreading on clean seawater

<b>t (s)</b>	<b>R (mm)</b>	<b>h (μm)</b>	<b>ln(h<sub>t</sub>)</b>	<b>ln(R)</b>	<b>ln(t)</b>
0.00±0.00	45±0	2322±22			
0.17±0.03	76±14	862±294	6.72±0.36	4.33	-1.77
0.28±0.02	93±9	553±107	6.30±0.21	4.53	-1.29
0.39±0.01	105±10	436±81	6.07±0.20	4.65	-0.94
0.43±0.00	109±4	403±31	6.00±0.08	4.69	-0.84
0.50±0.03	122±9	321±51	5.76±0.16	4.80	-0.69
0.62±0.02	133±11	268±47	5.58±0.17	4.89	-0.48
0.71±0.04	152±3	203±12	5.31±0.06	5.02	-0.34
0.81±0.01	165±3	173±10	5.15±0.06	5.11	-0.22
0.92±0.03	178±3	149±8	5.00±0.05	5.18	-0.08
1.00±0.02	187±6	134±9	4.90±0.07	5.23	0.00
1.11±0.03	197±11	122±14	4.80±0.12	5.28	0.10
1.28±0.04	216±3	101±5	4.62±0.05	5.37	0.24
1.44±0.05	234±10	86±7	4.45±0.09	5.45	0.37
1.67±0.03	253±13	74±8	4.30±0.11	5.53	0.51
1.88±0.19	262±10	69±6	4.23±0.09	5.57	0.63
1.83±0.08	266±21	67±12	4.20±0.17	5.59	0.60
2.02±0.01	279±21	61±10	4.10±0.17	5.63	0.70
2.20±0.07	304±13	51±5	3.93±0.09	5.72	0.79
2.31±0.04	311±12	49±5	3.88±0.09	5.74	0.84

2.45±0.03	329±13	44±4	3.77±0.09	5.80	0.90
2.66±0.12	348±22	39±5	3.66±0.13	5.85	0.98
2.69±0.01	356±22	38±5	3.62±0.13	5.88	0.99
2.80±0.02	363±14	36±3	3.58±0.07	5.89	1.03
2.93±0.03	373±11	34±2	3.52±0.06	5.92	1.07
3.09±0.08	383±8	32±1	3.47±0.05	5.95	1.13
3.27±0.05	396±20	30±3	3.41±0.11	5.98	1.18
3.45±0.03	400±15	29±2	3.38±0.07	5.99	1.24
3.71±0.04	413±16	28±2	3.32±0.09	6.02	1.31
3.82±0.06	415±20	28±3	3.31±0.10	6.03	1.34
3.95±0.01	417±15	27±2	3.30±0.08	6.03	1.37
4.13±0.06	428±12	26±2	3.25±0.07	6.06	1.42
4.44±0.06	436±9	25±1	3.22±0.07	6.08	1.49
4.88±0.04	442±9	24±1	3.19±0.06	6.09	1.58
5.20±0.12	449±9	23±1	3.18±0.06	6.11	1.65
5.78±0.14	454±12	23±1	6.72±0.36	6.12	1.75

**Table A6:** Kinetics data for ANS spreading on seawater (camera: continuous drive)

t(s)	R#1 (mm)	R#2 (mm)	Ave R (mm)	stdev	h ( $\mu\text{m}$ )	ln( $h_t$ )	ln(R)	ln(t)
0	45.0	45.0	45.0		2296			
0.30	89.4	89.4	89.5	0.0	581	6.36	4.49	-1.20
0.63	140.2	140.2	140.3	0.0	236	5.47	4.94	-0.46
0.91	172.0	172.0	172.0	0.0	157	5.06	5.15	-0.09
1.32	203.8	203.8	203.8	0.0	112	4.72	5.32	0.28
1.54	235.5	235.5	235.5	0.0	84	4.43	5.46	0.43
1.86	267.3	267.3	267.3	0.0	65	4.18	5.59	0.62
2.15	292.7	292.7	292.7	0.0	54	3.99	5.68	0.77
2.47	318.1	318.1	318.1	0.0	46	3.83	5.76	0.90
2.76	343.5	343.5	343.5	0.0	39	3.67	5.84	1.02
3.06	368.9	368.9	368.9	0.0	34	3.53	5.91	1.12
3.38	394.3	394.3	394.3	0.0	30	3.40	5.98	1.22
3.69	413.3	413.3	413.3	0.0	27	3.30	6.02	1.31
4.00	422.8	422.8	422.8	0.0	26	3.26	6.05	1.39
4.31	432.4	429.2	430.8	2.2	25	3.22	6.07	1.46
4.63	438.7	435.5	437.1	2.2	24	3.19	6.08	1.53
4.95	441.9	438.7	440.3	2.2	24	3.18	6.09	1.60
5.25	448.2	445.1	446.6	2.2	23	3.15	6.10	1.66
5.57	451.4	448.2	449.8	2.2	23	3.13	6.11	1.72

5.88	454.6	451.4	453.0	2.2	23	3.12	6.12	1.77
6.19	457.8	457.8	457.8	0.0	22		6.13	1.82

**Table A7:** Kinetics data (Ave±Stdev) for ANS spreading on seawater with a surface film

(\* represents a single time point see text for details)

t(s)	R (mm)	h (μm)	ln(h <sub>t</sub> )	ln(R)	ln(t)
0.00±0.00	45±0	2343±0			
1.21±0.00	54±1	1620±34	7.39±0.02		
1.50±0.00	56±1	1529±31	7.33±0.02	3.99	0.19
1.82±0.00	57±1	1445±29	7.28±0.02	4.02	0.41
2.42±0.01	60±1	1315±49	7.21	4.05	0.60
2.71±0.01	62±1	1248±45	7.18±0.04	4.10	0.88
3.01±0.01	63±1	1201±21	7.13±0.04	4.12	1.00
3.47±0.20	64±1	1143±20	7.09±0.02	4.14	1.10
4.30±0.10	66±0	1075±0	7.04±0.02	4.17	1.24
5.29±0.21	68±1	1014±17	6.98	4.20	1.46
6.20±0.21	70±0	957±0	6.92±0.02	4.23	1.66
7.39±0.21	73±1	896±28	6.86	4.25	1.82
9.06±0.00	75±1	836±19	6.80±0.03	4.29	2.00
11.04±0.64	78±2	782±34	6.73±0.02	4.32	2.20
15.26±0.21	84±1	665±22	6.66±0.04	4.36	2.40
13.60±0.44	71±1	729±20	6.50±0.03	4.44	2.73
15.26±0.21	83±1	681±9	6.59±0.03	4.39	2.61
19.68±0.81	88±0	615±0	6.52±0.01	4.42	2.73
26.11±1.04	94±2	529±19	6.42±0.00	4.48	2.98

29.87±1.08	97±1	509±12	6.29±0.04	4.54	3.26
33.26±1.14	99±1	484±11	6.23±0.02	4.57	3.40
38.69±0.93	103±3	448±29	6.18±0.02	4.59	3.50
42.81±1.24	106±4	425±32	6.10±0.07	4.63	3.66
*46.64	106	421	6.05±0.07	4.66	3.76
*50.90	109	403	6.04	4.66	3.84
*56.67	112	380	6.00	4.69	3.93
60.74±1.38	117±4	348±23	5.94	4.72	4.04
76.05±2.04	127±6	295±29	5.85±0.07	4.76	4.11
91.07±1.90	134±7	266±27	5.68±0.10	4.85	4.33
106.01±1.99	139±7	245±24	5.58±0.10	4.90	4.51
121.01±1.99	146±6	224±17	5.50±0.10	4.94	4.66
135.98±1.97	151±6	209±17	5.41±0.08	4.98	4.80
151.05±1.99	156±6	196±16	5.34±0.08	5.02	4.91
165.99±1.99	161±8	184±18	5.28±0.08	5.05	5.02
196.08±1.88	168±6	168±12	5.21±0.10	5.08	5.11
*227.41	170	163		5.13	5.28

**Table A8:** Kinetics data (Ave±Stdev) for IFO 120 spreading on clean seawater (\* represents a single time point see text for details)

t(s)	R (mm)	h (µm)	ln[(h <sub>t</sub> )	ln(R)	ln(t)
0.00	45±0	2379±16			
0.26±0.05	58±3	1416±172	7.25±0.12	4.07	-1.37
*0.60	72	934	6.83	4.28	-0.51
0.87±0.05	78±9	800±177	6.55±0.05	4.36	-0.15
1.17±0.06	89±11	616±150	6.25±0.04	4.49	0.16
1.48±0.06	102±11	470±100	6.08±0.12	4.63	0.39
1.78±0.05	112±16	398±108	5.85±0.11	4.72	0.57
2.03±0.01	124±16	319±78	5.67±0.13	4.82	0.71
2.45±0.06	135±18	269±69	5.48±0.12	4.91	0.89
2.68±0.04	148±18	224±53	5.31±0.11	5.00	0.99
3.00±0.05	161±18	190±41	5.11±0.05	5.08	1.10
3.30±0.06	177±13	155±23	5.00±0.09	5.17	1.19
3.61±0.05	186±18	141±26	4.87±0.09	5.23	1.28
3.80±0.19	197±15	126±18	4.76±0.05	5.28	1.33
4.23±0.06	205±9	115±9	4.68±0.01	5.32	1.44
4.51±0.03	215±4	104±4	4.62±0.01	5.37	1.51
4.84±0.08	224±9	96±7	4.53±0.03	5.41	1.58
5.16±0.05	231±9	91±6	4.48±0.03	5.44	1.64
5.45±0.04	237±9	86±6	4.41±0.01	5.47	1.69

5.77±0.06	247±10	79±6	4.30±0.02	5.51	1.75
*6.08	256	73	4.20	5.55	1.81
*6.35	269	66	4.10	5.59	1.85
6.72±0.08	280±2	61±1	4.07±0.08	5.63	1.90
7.65±0.10	298±6	54±2	3.95±0.03	5.70	2.03
8.63±0.09	316±12	48±3	3.80±0.04	5.75	2.15
9.41±0.35	339±9	42±2	3.66±0.06	5.83	2.24
10.55±0.13	359±1	37±0	3.56±0.10	5.88	2.36
11.53±0.12	378±7	34±1	3.45±0.13	5.94	2.44
13.68±0.09	405±4	29±1	7.25±0.12	6.00	2.62
*14.64	415	28	6.83	6.03	2.68
17.71±0.05	434±0	26±0		6.07	2.87

**Table A9:** Kinetics data (Ave $\pm$ Stdev) for IFO 120 spreading on seawater with surface film (\*represents a single time point see text for details)

<b>t (s)</b>	<b>R (mm)</b>	<b>h (<math>\mu</math>m)</b>	<b>ln(h<sub>t</sub>)</b>	<b>ln(R)</b>	<b>ln(t)</b>
0 $\pm$ 0	45 $\pm$ 0	2388 $\pm$ 34			
15 $\pm$ 0	54 $\pm$ 4	1615 $\pm$ 168	0.48 $\pm$ 0.10	3.99	2.71
*25	54	1730	0.57	3.98	3.22
63 $\pm$ 7	59 $\pm$ 4	1425 $\pm$ 212	0.33 $\pm$ 0.12	4.07	4.14
*167	61	1354	0.28 $\pm$ 0.30	4.12	5.11
287 $\pm$ 16	66 $\pm$ 10	1134 $\pm$ 336	0.10 $\pm$ 0.30	4.19	5.66
514 $\pm$ 35	73 $\pm$ 6	927 $\pm$ 160	-0.11 $\pm$ 0.21	4.29	6.24
663 $\pm$ 7	85 $\pm$ 9	700 $\pm$ 146	-0.41	4.44	6.50
*767	86	700	-0.40 $\pm$ 0.16	4.45	6.64
887 $\pm$ 16	92 $\pm$ 22	626 $\pm$ 274	-0.40 $\pm$ 0.44	4.52	6.79
982 $\pm$ 19	87 $\pm$ 8	638 $\pm$ 105	-0.52 $\pm$ 0.45	4.47	6.89
1127 $\pm$ 16	106 $\pm$ 27	476 $\pm$ 210	-0.51 $\pm$ 0.24	4.66	7.03
1254 $\pm$ 17	112 $\pm$ 20	413 $\pm$ 135	-1.00	4.72	7.13
1367 $\pm$ 16	120 $\pm$ 31	367 $\pm$ 165	-0.79 $\pm$ 0.46	4.79	7.22
1487 $\pm$ 16	128 $\pm$ 33	318 $\pm$ 136	-0.97 $\pm$ 0.34	4.86	7.30
1594 $\pm$ 25	135 $\pm$ 24	278 $\pm$ 79	-1.06 $\pm$ 0.46	4.90	7.37
1727 $\pm$ 16	145 $\pm$ 34	249 $\pm$ 93	-1.19 $\pm$ 0.44	4.97	7.45
1863 $\pm$ 7	166 $\pm$ 15	181 $\pm$ 25	-1.38 $\pm$ 0.31	5.11	7.53
*1978	186	143	-1.43 $\pm$ 0.38	5.23	7.59

2087±16	170±37	168±64	-1.88±0.10	5.14	7.64
2194±25	177±26	155±44	-1.95	5.18	7.69
2327±16	185±37	142±53	-1.82±0.39	5.22	7.75
2454±17	194±25	133±35	-2.05±0.39	5.27	7.81
*2555	176	153	-1.99±0.38	5.17	7.85
*2675	185	137	-2.23±0.41	5.22	7.89
2782±19	204±18	125±14	-1.88	5.32	7.93
2915	198	122	-1.99	5.29	7.98
3052±29	219±21	107±11	-2.43±0.59	5.39	8.02
*3155	213	105	-2.11	5.36	8.06
3287±16	237±23	87±13	-2.66±0.71	5.47	8.10
*3368	248	82	0.48±0.10	5.52	8.12
*3668	262	77	0.57	5.57	8.21
*4268	295	57		5.69	8.36

**Table A10:** Average HC levels in water samples collected 6 m from oil release.

	ANS with Dispersant			ANS with no Dispersant			ANS (Surface Film) with Dispersant		
	Ave ± Stdev (mg/L)			Ave ± Stdev (mg/L)			Ave ± Stdev (mg/L)		
Time	Depth			Depth			Depth		
(min)	5cm	75 cm	145cm	5cm	75 cm	145cm	5cm	75 cm	145cm
0									
5	42.3±3.7	37.6±29.1	4.1±1.1	2.8			13.0±13.7	17.6±12.1	3.1
15	17.0±6.9	16.7±8.8	10.3±7.3				12.2±2.0	17.0±3.7	6.6±5.8
30	13.2±1.0	13.3±1.5	9.7±2.9				11.3±0.8	13.4±2.3	6.1±5.4
45	8.5±5.6	9.5±0.9	8.3±1.6				10.3±1.4	11.2±0.2	5.7±3.6
60	9.0±1.9	9.2±1.0	7.6±1.4				9.5±1.7	10.3±0.4	7.8±2.4
75	7.2±1.9	7.6±0.7	7.4±1.1				12.4±2.5	8.1±0.7	7.7±1.6
90	8.6±2.6	8.2±1.0	7.2±1.4				10.1±1.5	8.3±1.1	6.1±1.9

**Table A11:** Average HC levels in water samples collected 10 m from oil release.

	ANS with Dispersant			ANS with no Dispersant			ANS (Surface Film) with Dispersant		
	Ave $\pm$ Stdev (mg/L)			Ave $\pm$ Stdev (mg/L)			Ave $\pm$ Stdev (mg/L)		
Time	Depth			Depth			Depth		
(min)	5cm	75 cm	145cm	5cm	75 cm	145cm	5cm	75 cm	145cm
0									
5	24.8 $\pm$ 22.8	27.1 $\pm$ 21.7	3.8 $\pm$ 0.2	14. $\pm$ 13.3	5.9 $\pm$ 1.2		67.9 $\pm$ 23.7	63.5 $\pm$ 53.8	6.4 $\pm$ 4.1
15	20.4 $\pm$ 5.4	16.1 $\pm$ 6.0	16.0 $\pm$ 2.2	2.6	3.3 $\pm$ 0.1	2.8	37.6 $\pm$ 8.5	36.5 $\pm$ 11.6	10.1 $\pm$ 10.1
30	17.6 $\pm$ 5.0	13.7 $\pm$ 2.2	12.8 $\pm$ 3.5	3.0 $\pm$ 0.9	2.9 $\pm$ 0.8	2.3 $\pm$ 0.7	21.9 $\pm$ 1.7	24.3 $\pm$ 5.6	9.1 $\pm$ 7.1
45	12.0 $\pm$ 0.6	12.0 $\pm$ 1.6	12.3 $\pm$ 1.4	3.8	2.5 $\pm$ 0.3	2.7	16.7 $\pm$ 0.4	16.1 $\pm$ 2.2	10.9 $\pm$ 6.7
60	10.0 $\pm$ 0.0	9.9 $\pm$ 0.1	10.3 $\pm$ 2.2	2.2	2.5	2.9 $\pm$ 0.4	13.6 $\pm$ 3.2	13.1 $\pm$ 2.8	11.7 $\pm$ 2.0
75	10.8 $\pm$ 1.1	9.0 $\pm$ 1.4	9.1 $\pm$ 1.7	2.5	2.7 $\pm$ 0.3	3.1	13.1 $\pm$ 2.6	11.0 $\pm$ 3.1	11.8 $\pm$ 2.6
90	9.8 $\pm$ 2.4	6.9 $\pm$ 1.4	8.2 $\pm$ 2.7		2.5	2.2	12.2 $\pm$ 2.7	9.9 $\pm$ 1.0	10.0 $\pm$ 2.3

**Table A12:** Average interfacial tension in water samples collected 6 m from oil release.

	ANS with Dispersant			ANS with no Dispersant			ANS (Surface Film) with Dispersant		
	Ave±Stdev (Dynes/cm)			Ave±Stdev (Dynes/cm)			Ave±Stdev (Dynes/cm)		
Time	Depth			Depth			Depth		
(min)	5cm	75 cm	140cm	5cm	75 cm	140cm	5cm	75 cm	140cm
0	75.1±0.3	74.9±0.1	74.9±0.2						
5	70.7±5.0	67.4±7.4	75.0±0.2	71.6±1.2	73.9±1.1	74.4±1.3	54.6±3.5	58.7±1.7	74.4±0.6
15	72.0±2.3	72.4±2.3	73.3±2.4	74.4±1.2	74.4±1.3	74.5±1.3	62.7±0.6	64.7±2.1	71.7±4.7
30	72.2±0.3	73.5±1.4	71.3±1.3	74.4±1.1	74.4±1.1	74.6±1.3	65.1±2.2	64.0±1.8	71.7±5.1
45	73.6±1.0	72.2±0.8	72.8±1.0	73.9±1.0	73.9±0.8	74.1±0.9	65.7±2.4	66.9±1.5	71.2±2.0
60	72.7±1.7	74.0±0.9	73.4±1.4	74.4±1.1	74.3±1.1	73.5±0.6	69.1±1.7	68.7±2.6	69.5±3.0
75	72.6±2.2	72.7±0.3	73.9±1.2	74.0±0.8	74.5±1.1	74.4±1.1	68.0±1.5	68.5±1.7	69.9±1.2
90	71.9±0.3	71.6±2.4	72.0±2.3	73.5±1.1	74.1±0.9	74.5±1.1	67.0±2.5	68.0±1.0	70.2±1.6

**Table A13:** Average interfacial tension in water samples collected 10 m from oil release.

	ANS with Dispersant			ANS with no Dispersant			ANS (Surface Film) with Dispersant		
	Ave±Stdev (Dynes/cm)			Ave±Stdev (Dynes/cm)			Ave±Stdev (Dynes/cm)		
Time	Depth			Depth			Depth		
(min)	5cm	75 cm	140cm	5cm	75 cm	140cm	5cm	75 cm	140cm
0	75.0±0.2	74.9±0.2	74.7±0.4						
5	67.6±4.1	66.3±5.7	75.0±0.1	74.3±1.2	73.7±1.2	74.3±1.1	60.6±7.5	65.7±6.6	74.9±0.4
15	71.1±4.2	71.5±3.6	73.0±3.0	74.3±1.3	74.4±1.1	74.4±1.2	59.4±5.4	62.0±4.0	71.9±4.1
30	73.1±2.4	72.6±1.6	72.4±3.3	74.2±1.1	74.4±1.1	74.3±1.2	64.1±6.3	63.5±5.0	65.5±8.2
45	73.2±1.9	71.7±4.0	72.8±1.1	74.4±1.3	74.4±1.3	74.4±1.2	67.6±3.1	65.6±1.5	71.±4.0
60	73.5±1.5	74.3±1.0	73.9±1.1	74.2±1.0	74.5±1.2	74.4±1.1	66.4±3.9	66.7±0.5	66.7±0.5
75	73.8±1.0	73.8±1.3	74.0±1.2	74.0±1.1	74.4±1.2	74.4±1.1	65.5±4.1	68.9±2.6	66.3±1.3
90	74.0±0.9	74.3±1.1	73.4±1.3	74.4±1.1	74.4±1.3	74.2±1.5	65.6±2.0	68.3±2.8	66.5±0.6

**Appendix B**  
**Example Calculations**

## Example Calculations

### Example 1 (Chapter 3.3)

$V = \pi r^2 h_o$  (5) This is the equation for the volume of a cylinder, which represents the oil containment barrier.  $V$  is the volume of oil,  $\pi$  is a constant of 3.14,  $r$  is the radius which is  $\frac{1}{2}$  the diameter of the oil containment barrier, and  $h$  is the oil thickness. By rearranging the equation, we can determine oil thickness.

$h_o = \frac{V}{\pi r^2}$  Knowns are as follows: Volume of oil is 15 cm<sup>3</sup>, diameter of containment ring is 9.0 cm therefore the radius is 4.5 cm.

$$h_o = \frac{15\text{cm}^3}{\pi 4.5\text{cm}^2} = 0.24\text{cm} = \underline{2.4\text{mm}}$$

### Example 2 (Chapter 4.3)

$\gamma(t) = \gamma_o - 2RTC_o\sqrt{\frac{Dt}{\pi}}$  (6) where  $\gamma(t)$  and  $\gamma_o$  are the surface tension at time ( $t$ ) and initial surface tension respectively,  $R$  is the ideal gas constant,  $T$  is the temperature in degrees Kelvin,  $C_o$  is the surfactant concentration, and  $D$  is the diffusion coefficient. For short-time limit adsorption, a linear relationship exists between  $\gamma(t)$  and  $\sqrt{t}$  which is illustrated in Figure 9 for ALC and ANS.

Knowns for ANS are as follows: a plot of  $\gamma(t)$  versus  $\sqrt{t}$  produced a slope of  $-6.08 \times 10^{-7}$

$\text{Ncm}^{-1}\text{s}^{-1/2}$  ( $\text{slope} = -2RTC_o\sqrt{\frac{D}{\pi}}$ ),  $C_o$  is the surfactant concentration taken as asphaltenes,

$R$  is the gas constant ( $8.31 \times 10^2 \text{ cmN}^\circ\text{K}^{-1}\text{mol}^{-1}$ ), and  $D$  is the diffusion coefficient which

can be determined from the slope of the line. To determine  $C_o$  the following was considered:

- 1) The average mass of ANS used in the diffusion study was 12.73 grams.
- 2) The asphaltenes present in ANS was 4.3% by mass.
- 3) Therefore the mass of asphaltenes in ANS are  $12.73 \text{ g} \times 0.043 = 0.547 \text{ g}$ .
- 4) Total volume of seawater used was 20L or  $\text{m}^3$ .
- 5) Average Temperature was  $20.8 \text{ }^\circ\text{C}$  or 294 degree Kelvin ( $^\circ\text{K}$ ).
- 6) Assume an average molecular weight of 5000 g/mol for asphaltenes.

$$\text{Therefore } C_o = \frac{m}{V} = \frac{0.547 \text{ g}}{20 \text{ L}} = 0.0274 \text{ g/L} = \frac{0.0274 \text{ g/l}}{5000 \text{ g/mol}} = 5.47 \times 10^{-6} \text{ mol/L}$$

$$C_o = 5.47 \times 10^{-6} \text{ mol/L} \times \frac{1.00 \text{ L}}{1000 \text{ cm}^3} = 5.47 \times 10^{-9} \text{ mol/cm}^3$$

To determine the Diffusion Coefficient ( $D$ ):

$$\text{slope} = -2RTC_o \sqrt{\frac{D}{\pi}} \quad \text{rearranging the equation produces,}$$

$$\frac{\text{slope}}{RTC_o} = -\sqrt{\frac{D}{\pi}} = \frac{-6.08 \times 10^{-7} \text{ Ncm}^{-1} \text{ s}^{-1/2}}{2 \times 8.31 \times 10^2 \text{ cmN}^\circ \text{ Kmol}^{-1} \times 294^\circ \text{ K} \times 5.47 \times 10^{-9} \text{ mol/cm}^3} = -\sqrt{\frac{D}{\pi}}$$

$$D = \underline{1.62 \times 10^{-7} \text{ cm}^2 / \text{s}}$$

**Example 3 (Chapter 4.5 see Table 4 ANS-SF)**

$$\ln(m_t) = \ln(m_0) - kt \quad (11) \text{ calculating values from left side of equation.}$$

Know values are as follows:

1.  $t=5 \text{ min}$  (all data from Table 4).
2.  $m_0$  is the initial mass of 258.7grams at  $t=0 \text{ min}$ .

3.  $m_t$  is the mass at time  $t = 5$  min. which is 0.0459 grams.

4.  $m_{ss}$  is the mass at steady-state or terminal mass at  $t = 90$  min., which is 0.0107 grams.

$$\ln(m_t) = \ln(m_0) - kt = \ln(0.0459) = \ln(m_0) - kt$$

$$\ln[0.0459] = -kt = \underline{-3.08} = \ln(m_0) - kt$$

The values calculated on the left side of the equation were plotted as a function of  $t$  to produce a linear graph (Figure 16) and the slope is equal to  $-k$ .

#### **Example 4 (Chapter 4.5)**

Let  $x_1$  equal the rate coefficient for dispersed ANS with a horizontal interfacial gradient.

Let  $x_2$  equal the rate coefficient for dispersed ANS in clean seawater.

$$\% \text{ Difference} = \left| \frac{x_1 - x_2}{\frac{(x_1 + x_2)}{2}} \right| \times 100\% = \left| \frac{0.0157 - 0.0098}{\frac{(0.0157 + 0.0098)}{2}} \right| \times 100\% = \underline{46\%}$$